Feasibility study of ghost hits reduction in Silicon Vertex Detector for Belle II experiment

by

Kun Wan

Submitted to the Department of Physics
in partial fulfillment of the requirements for the degree of

Master of Science

at the

The University of Tokyo

September 2017

Certified by.....
Hiroaki Aihara
Professor
Thesis Supervisor

Feasibility study of ghost hits reduction in Silicon Vertex Detector for Belle II experiment

by

Kun Wan

Submitted to the Department of Physics
on July 6th, 2017, in partial fulfillment of the
requirements for the degree of
Master of Science

Abstract

Belle II experiment is a next generation B-factory that is aimed to study many exciting and intriguing topics in the research of New Physics, located in Tsukuba, Japan. It is expected to collect around 50 times more data than its predecessor, Belle, mostly thanks to 40 times higher luminosity provided by SuperKEKB over the original KEKB accelerator, which naturally raises the new requirements on both hardware and software in detector. SVD is composed of 4 layers strip detectors in Belle II for spatial precise tracking and vertex fitting. Its excellent performance is extremely important to the success of Belle II.

In this thesis, the feasibility study of using charge correlation on P and N types of semiconductor to reject the ghost hits will be presented. It will mainly benefits the correct vertexing of particles decay and fast filtering in SuperKEKB environment. The general information and the significance of Belle II experiment will be introduced in Chapter 1. In order to have a comprehensive understanding of this topic, both hardware and tracking software features about SVD are instructively implemented in chapter 2 and 3. For closely approaching the real experiment, beam test data was taken in DESY using one SVD ladder at 2$\sim$6 GeV beam energy. A few observable quantities like asymmetry of P&N charges are studied to searching for a formula of hits purity, presenting probability of a hit being real. These relative content will be illustrated in Chapter 4 and 5. As the beneficial outcome of this study, the correctness of SVD simulation of charge sharing on floating strips is largely improved, contributing to the offline calibration of SVD clusters. All relative work and results will be included as part of SVD group contribution in Belle II.

Thesis Supervisor: Hiroaki Aihara
Title: Professor

Acknowledgments

I would first like to thank my thesis advisor Prof. Hiroaki Aihara of the Department of Physics. He consistently allowed this paper to be my own work, but steered me in the right the direction whenever he thought I needed it. Secondly, I thank Assistant Professor Yoshiyuki Onuki, for guiding me participated in the work of SVD and relentlessly driving to optimize my research details with his thorough understanding in relative works.

I would also like to thank the experts who were involved in the validation survey for this research project: Associate Professor Takeo Higuchi, and many members in Belle II collaboration especially those in SVD L6 group. Without their passionate participation and input, the validation survey could not have been successfully conducted. I also very much appreciate the help and supervision from SVD software group for imparting knowledge of software analysis by their excellent contribution towards Belle II.

In the end, I would be always be grateful for my parents and friends who care and support my every decision no matter where I am. It is them who give me courage and strength to conquer all.

Contents

List of Figures

List of Tables

Chapter 1

Experiment Introduction

1.1 Belle II experiment

For the past several decades, the success of the Standard Model has always been regarded as one of the greatest achievements in not only physics, but science in general, which predicted the existence of hundreds of new particles and gave a quite precise description of fundemental interactions except for Gravity. There's a moment that physicists even consider that they are almost close to the stage when science came to a cross road before the discovery of Relativity in 1905. However, the universe once again proves its unimaginable profundity by revealing some anomaly in the Standard Model[1]. Thanks to the development of technology, physicists can push the human vision into a land that we never expect before, and so, a bunch of new discovery that do not fit into the Standard Model come out, driving us into the searching for new physics, expecting a better framwork can explain the very fundament of the world.

In many potential topics of searching for new physics, the study of CP violation draws a special attention of many particle physicists. As the prediction of CP violation from the Standard Model[2] is much smaller than the experimental examinations which are confirmed by many experiments[3]. In particular, the B meson system shows a quite large trace of finding such violation[4]. The Belle experiment was constructed and run since 1999 for around 10 years by colliding the beam of electron and position from KEKB accelerator. During its working time, located in

Tsukuba, Japan. Over 1000 fb^{-1} data was collected and it notably contributes to the confirmation of CP violation mechanism, honored by Nobel Prize Committe in 2008[5].

The Belle experiment's success is significant but not fully exploited yet. There are still many topics waiting for being studied and many hints remains beyond the reach of Belle technology design and actual performance. Inherited from the collaboration of Belle experiment, Belle II was formed in 2008 in order to continue extend the researches in this field. The upgraded powerful collider, SuperKEKB is being prepared in a luminosity of $8 \times 10^{34}\ cm^{-2}s^{-1}$, 40 times higher than its predecessor KEKB. The enhanced performance is aimed to find the trace of new physics which is not possible statistically in Belle due to its data mount. It is the world most bright machine and make Belle II the most precise-frontier experiment in the world.

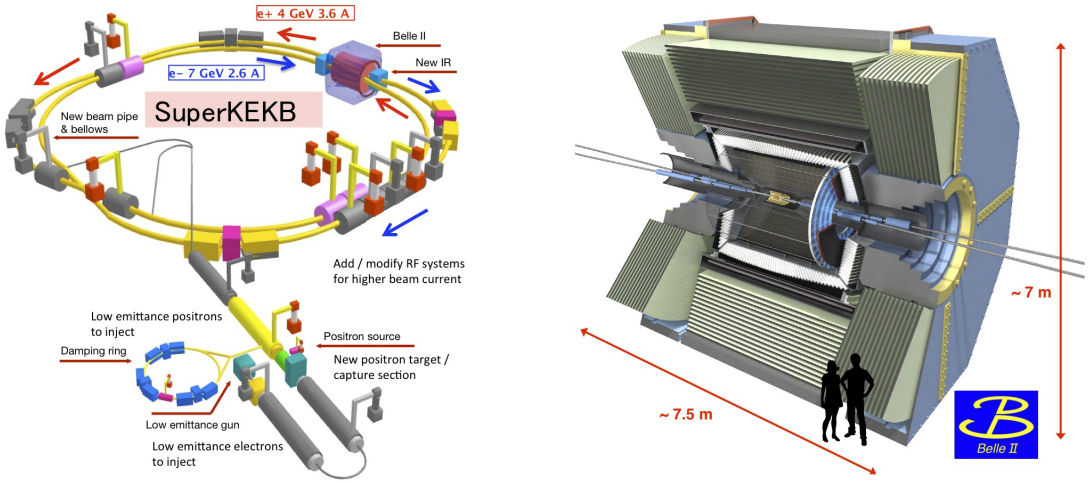

Figure 1-1: KEK is upgrading its B-factory to the SuperKEKB facility (left) to provide a 40-fold increase in instantaneous luminosity by exploiting higher beam currents, a large crossing-angle and squeezing the beams down to nano meter scales. Also the former Belle detector needs to be upgraded to Belle II (right) to cope with the enormous increase in intensity.

Belle II is a highly coped and finely designed detector which contains series of detectors with different speciality. Silicon vertex detectors (SVD) is composed of 4 layers strip detectors that are designed for precise tracking of high level triggering and vertex fitting, and it is located in the second closest to the interaction point (IP)

of SuperKEKB. Another 2 layers pixel detectors (PXD) is installed between SVD and IP. All 6 layers of these Vertex detectors (called VXD) are constructed by different groups of people in Japan, Itali, Australia, India and Austria.

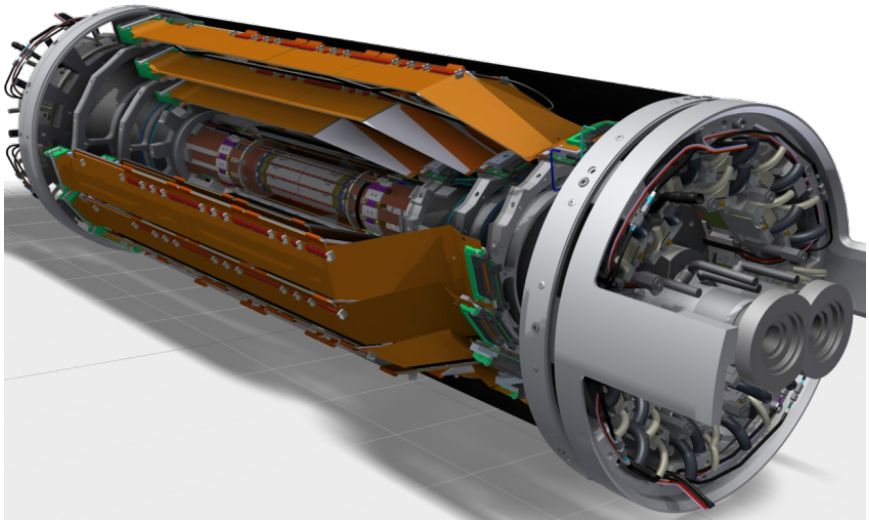

Figure 1-2: VXD including PXD, SVD and supporting structure

In order to work perfectly with SuperKEKB upgrade, the design of the Belle II SVD inherits the good characteristics of the Belle vertex detector and beyond: low mass, high precision, immunity to background hits, radiation tolerance and long-term stability. It is designed with silicon strip sensors to avoid the huge channel count of pixels without compromising the vertex-detection capability of Belle II.

The high quality of SVD is essential for the success of whole project. The SVD is responsible for the extreme fine track and vertex reconstruction of primary particles like B meson s whose mean lifetime is of transience in 10^{-12} s. To assure SVD's capability of performing good tracking, mechanical design, production and alignment are carefully taken by experts, as well as its tracking software development, which directs me into SVD massive production and research for potential optimization of tracking package during my master course.

1.2 Physics Motivation of Belle II

In many related researches around searching New Physics, the understanding of *CP* violation plays a role that may give an answer to the matter and anti-matter unbalance in the observed scale of universe. *CP* violation is the violation of *CP*-symmetry, often called just *CP*, which is the product of two symmetries: *C* for charge conjugation, which transforms a particle into its antiparticle, and *P* for parity, which creates the mirror image of a physical system. The strong interaction and electromagnetic interaction seem to be invariant under the combined *CP* transformation operation, but this symmetry is slightly violated during certain types of weak decay. Historically, *CP*-symmetry was proposed to restore order after the discovery of parity violation in the 1950s[6].

CP violation is allowed in the Standard Model if a complex phase appears in the CKM matrix describing quark mixing[2]. A necessary condition for the appearance of the complex phase is the presence of at least three generations of quarks. CKM (Cabbibo-Kobayashi-Maskawa) matrix is a matrix that is given by conducting two matrix of up and down types of quarks from mass eigenstate to flavour eigenstate. It basically shows the interaction coupling strength of a quark changing into another flavour shown like:

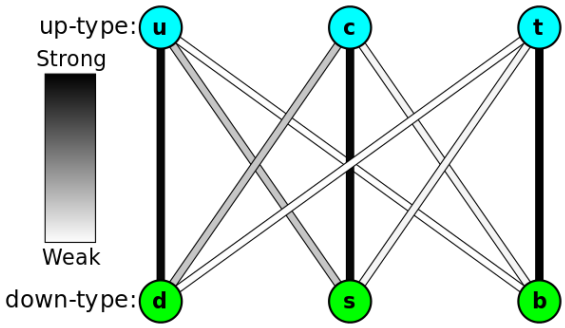

Figure 1-3: Quark weak interactions

CKM can expressed as below:

$$\begin{bmatrix} d' \\ s' \\ b' \end{bmatrix} = \begin{bmatrix} V_{ud} & V_{us} & V_{ub} \\ V_{cd} & V_{cs} & V_{cb} \\ V_{td} & V_{ts} & V_{tb} \end{bmatrix} \begin{bmatrix} d \\ s \\ b \end{bmatrix}$$

On the left is the weak interaction doublet partners of up-type quarks, and on the right is the CKM matrix along with a vector of mass eigenstates of down-type quarks. The CKM matrix describes the probability of a transition from one quark i to another quark j. These transitions probability are proportional to $|Vij|^2$.

And this is a real unitary matrix which stands for Lagrangian being Lorentz invariant. Currently, the most precise measurement of elements in this matrix is [7]:

$$\begin{bmatrix} |V_{ud}| & |V_{us}| & |V_{ub}| \\ |V_{cd}| & |V_{cs}| & |V_{cb}| \\ |V_{td}| & |V_{ts}| & |V_{tb}| \end{bmatrix} = \begin{bmatrix} 0.97427 \pm 0.00014 & 0.22536 \pm 0.00061 & 0.00355 \pm 0.00015 \\ 0.22522 \pm 0.00061 & 0.97343 \pm 0.00015 & 0.0414 \pm 0.00012 \\ 0.00886^{+0.00033}_{-0.00032} & 0.0405^{+0.0011}_{-0.0012} & 0.99914 \pm 0.00005 \end{bmatrix}$$

The significance of CKM matrix is that it predicts the existence of 3 generations of quark family instead of 2 out of the Standard Model accuracy of normal. It is rather interesting for the particle physicists that with the development of accelerators, experiment with large statistics becomes available, the direct or indirect measurement of *CP* violation does lead a new ground for extending the Standard Model and searching for New Physics.

Here is an example of illustrating the possible effect being found in Belle II experiment. The large data set from enhanced performance of Belle II brings it into reality for NP study. The real value of the Super B factory in its ability to perform measurements in all fields of heavy flavor physics, extending from B^0 meson decays to charm physics,lepton τ physics, spectroscopy, and pure electroweak measurements.

Usually, we use the following notices and angles to track down many observables in neutral B meson system:

$$A(\Delta t) = \frac{\Gamma(B^0(\Delta t) \to f_{CP}) - \Gamma(\bar{B}^0(\Delta t) \to f_{CP})}{\Gamma(B^0(\Delta t) \to f_{CP}) + \Gamma(\bar{B}^0(\Delta t) \to f_{CP})} = S \sin(\Delta m \Delta t) \qquad (1.1)$$

$$f_{CP} = J/\psi K_s \tag{1.2}$$

$$S = -\sin(2\phi_1) \tag{1.3}$$

In here the Δt and Δm are the difference of mean lifetime and mass between the two different mass eigenstates of B mesons. Above values can be measured not in single final state. Compared to the final state ϕK_s, this value of $S = \sin 2\phi_1$ differs in $\Delta S = \sin 2\phi_1^{\phi K_s} - \sin 2\phi^{J/\psi K_s} = 0.22 \pm 0.17$ [8]. The former decays proceed through $b \to s\bar{s}s$ underlying quark process, possible only through the loop processes from the SM (left), and the right through the gluino-down squark contribution. While the CKM matrix elements included in the amplitudes of these decays are approximately real, the possibility of B^0-$\bar{B}^0$ mixing before the decay introduces an additional factor of $e^{-2i\phi_1}$. Hence, the decay time distribution of both decays is sensitive to $\sin 2\phi_1$, and the difference in the value measured in the two decays is expected to vanish within small corrections, $S = 0.03 \pm^{0.001}_{0.004}$[9]. However, NP particles can contribute in the loop of $B^0 \to K_S$, as right, and change the expectation for S.

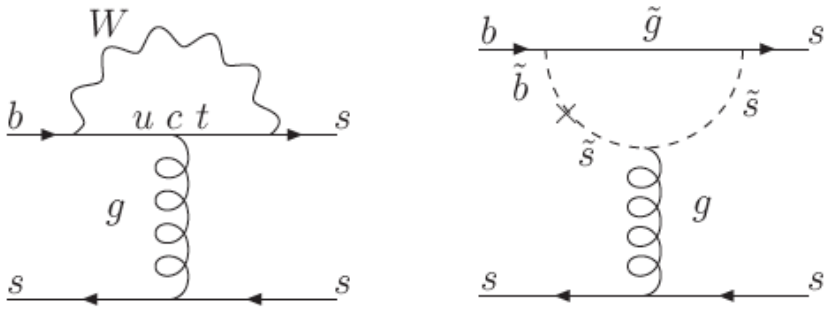

Figure 1-4: the SM contribution (left) and gluino down squark contribution (right)

And $B \to \phi K_S$ is one intermediate resonance of decay $B \to K_S K^+ K^-$, one can use a this decay to determine the value of S, which requires a very accurate $K_S K^+ K^-$ vertex reconstruction and background suppression. This is where Belle II can show its advantages. The sensitivity of this measurement to the luminosity can be seen in figure below:

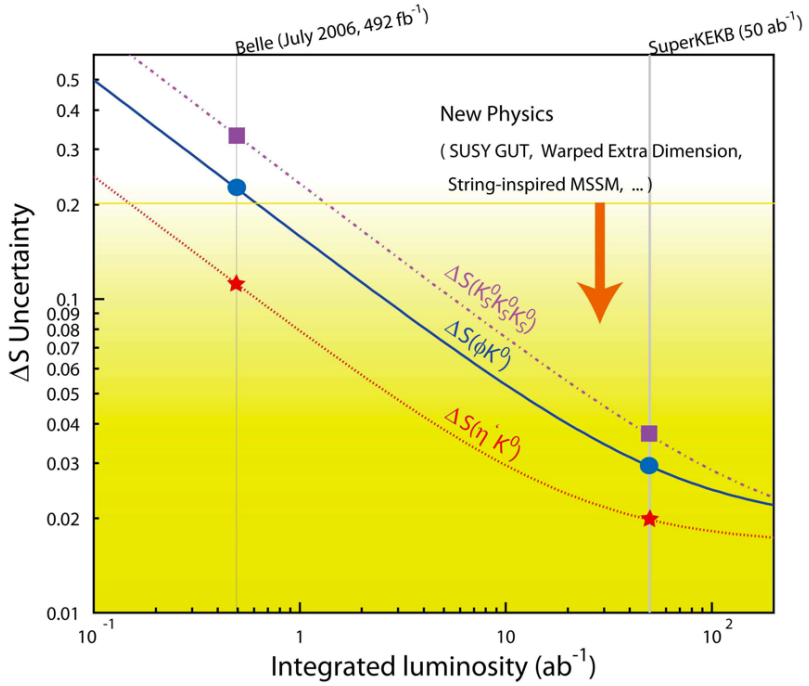

Figure 1-5: ΔS dependence of luminosity in expectation

1.3 SuperKEKB

In order to achieve such high luminosity, many methods has been carefully considered and conducted considered the experience from other experiments. The core scheme is called "Nano-Beam" [10] which is done by minimizing the longitudinal size of the overlap region of the two beams at the IP. The "hourglass" effects will suppress the value of β function of beam. The overlapped area of beam (d) is determined roughly by the horizontal beam size ϕ and horizontal half cross angle ${\sigma^*}_x$, see equation 1.5. This d is much smaller than the bunch length σ_z.

$$d \approx \frac{{\sigma^*}_x}{\phi} \tag{1.4}$$

The hourglass condition in the Nano-Beam scheme is expressed as:

$$\beta^*_y > d \tag{1.5}$$

To shorten d, a relatively large horizontal crossing angle and extremely small

horizontal emittances and horizontal beta functions at the IP for both beams are required. The luminosity of a collider is expressed by the following formula, assuming flat beams and equal horizontal and vertical beam sizes for two beams at the IP:

$$L = \frac{\gamma_{\pm}}{2er_e}\left(\frac{I_{\pm}\xi_{y\pm}}{\beta^*_{y\pm}}\right)\left(\frac{R_L}{R_{\xi_y}}\right) \tag{1.6}$$

where γ, e and r_e are the Lorentz factor, the elementary electric charge and the electron classical radius, respectively, R_L and R_{ξ_y} represent reduction factors for the luminosity and the vertical beam-beam parameter, which arise from the crossing angle and the hourglass effect. That leads the luminosity depending on three parameters out of the formula. The values for selected for three parameters and energy of beam with corresponding luminosity is shown below.[11]

		LER (e+)	HER (e-)	units
Beam Energy	E	4	7	GeV
Half Crossing Angle	ϕ	41.5		mrad
Horizontal Emittance	ε_x	3.2(2.7)	2.4(2.3)	nm
Emittance ratio	$\varepsilon_y/\varepsilon_x$	0.40	0.35	%
Beta Function at the IP	β^*_x/β^*_y	32 / 0.27	25 / 0.41	mm
Horizontal Beam Size	σ^*_x	10.2(10.1)	7.75(7.58)	μm
Vertical Beam Size	σ^*_y	59	59	nm
Betatron tune	ν_x/ν_y	45.530/45.570	58.529/52.570	
Momentum Compaction	α_c	2.74×10^{-4}	1.88×10^{-4}	
Energy Spread	σ_ε	$8.14(7.96) \times 10^{-4}$	$6.49(6.34) \times 10^{-4}$	
Beam Current	I	3.60	2.62	A
Number of Bunches/ring	n_b	2503		
Energy Loss/turn	U_0	2.15	2.50	MeV
Total Cavity Voltage	V_c	8.4	6.7	MV
Synchrotron Tune	ν_s	-0.0213	-0.0117	
Bunch Length	σ_z	6.0(4.9)	5.0(4.9)	mm
Beam-Beam Parameter	ξ_y	0.0900	0.0875	
Luminosity	L	8×10^{35}		$\mathrm{cm^{-2}s^{-1}}$

Figure 1-6: SuperKEKB parameters, values in parentheses denote parameters at zero beam currents

And for partially reduce the background directly from beam, the beam energy of electron pairs will be loosen from $E_{e^+} = 3.5\,GeV, E_{e^-} = 8\,GeV$ to $E_{e^+} = 4\,GeV, E_{e^-} = 7\,GeV$ so that the Lorentz boost factor from Lab to center of mass frame is reduced

from 0.43 to 0.28. By altering these parameters, the performance of SuperKEKB is listed in table below[11].

$$d \approx \frac{\sigma^*{}_x}{\phi} \tag{1.7}$$

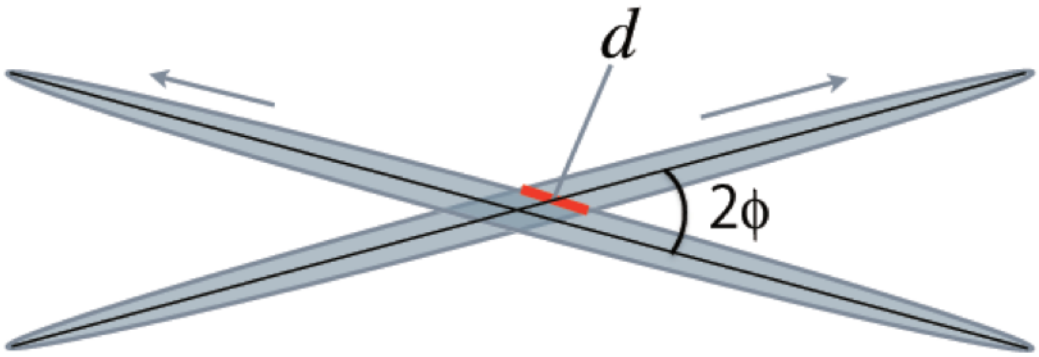

Figure 1-7: Beam crossing scheme

Table 1.1: beam parameters

Parameters	Values
Energy(GeV)	4.0/7.0
Current(A)	3.6/2.62
β_y^* (mm)	0.27/0.41
Luminosity ($10^{34} cm^{-2} s^{-1}$)	80
Crossing angle (mrad)	83
Perimeter of ring (km)	3

Chapter 2

Vertex Detectors in Belle II

In principle, the function of first a few layers of detectors is to perform the precise tracking in order to measure the decay vertices of B mesons. In Belle II experiment, vertex detectors including pixel detectors (PXD) and silicon vertex detectors (SVD) work for this purpose exclusively. Two sections of detectors are installed in Belle II orderly to meet the need of the different characteristics of beam and particle environment along with the growth of radius away from IP.

Table 2.1: PXD and SVD layers radius from IP and numbers of ladder.

Layer	1	2	3	4	5	6
Radius(mm)	14	22	38	80	104	135
Num of Ladders	8	12	7	10	12	16

2.1 Pixel Detector (PXD)

As we have illustrated before many times that the feature of SuperKEKB lays particular emphasis on its extreme high luminosity, and this raises the new demand on upgrading the detectors in Belle II.

Facing such severe hits rates, the closest structure is 2 layers of pixel detectors called PXD. The background majorly caused in related to beam can not only challenge the data taking but also damage the detectors, such as many photon-photon reaction and small transverse momentum (p_T) QED process.

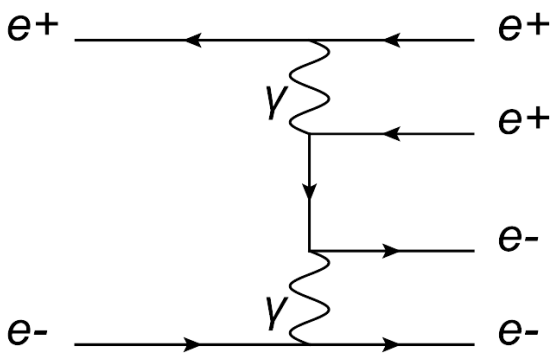

Figure 2-1: major source of double photon QED background in Belle II

The beam background rate can be roughly regarded as the inverse square of radius from the IP. In the nano-beam scheme, the cutoff of beam interaction region is only about 10 *mm* away from center. This is a good news for reconstruction of tracks and vertices but make the use of strip detectors in the first few layers impossible due to quite high occupancy, defined as the fraction of hit channels and total channels in every single triggered event.

Belle II takes DEPFET technology as the option for material of pixel sensors, because the low momentum range of particles requires lesser equipped amplifiers electronics and cooling system to avoid too much multiple scattering in reconstructing vertices of B meson decay.

Table 2.2: VXD Index, 1 and 2 are PXD, 3 to 6 are SVD

Layer	1	2	3	4	5	6
Radius(mm)	14	22	38	80	104	135
Num of Ladders	8	12	7	10	12	16

Table 2.3: PXD geometry

Index	num of Ladders	num of pixels $(z \times r\phi(\mu m^2))$	pixel size $(z \times r\phi(mm^2))$	sensitive region
Layer 1	8	768×250	55×50 60×50	44.8×12.5
Layer 2	12	768×250	70×50 85×50	6.44×12.5

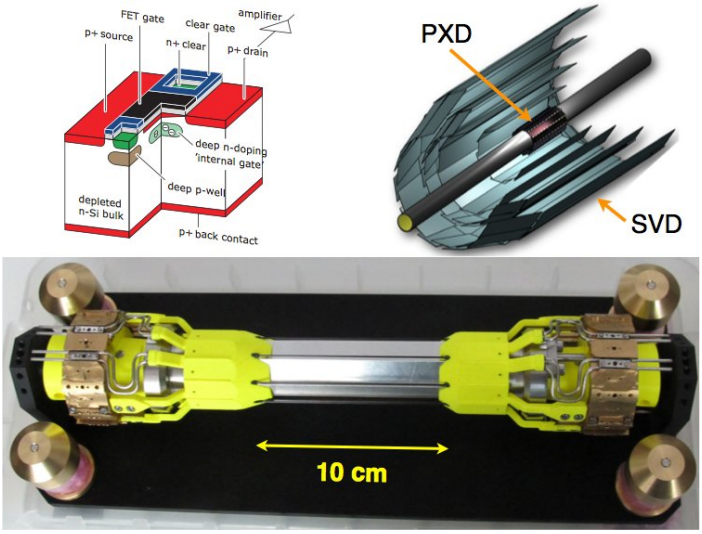

Figure 2-2: DEPFET and its silicon depleted structure

2.2 Silicon Vertex Detectors

Working with the inner component PXD and outside Central Drift Chamber (CDC), SVD performs the measurement of two decay vertices in B^0-$\bar{B}^0$ mixing-induced CP violation through precise tracking and reconstruction. In addition, SVD also serves for same purposes in D meson involved decay channels and τ lepton decay.

SVD is designed with silicon sensors of strip channels along with two sides, vertical and parallel to the beam direction. This is for reducing a huge amount of readout channels using pixel detectors without compromising the vertex ability of Belle II.

The structure of Belle II SVD can be illustrated as Fig 2-3. Since the SuperKEKB will collide the electron positron at energy of 7 GeV and 4 GeV respectively, the Lorentz boost will be $\beta\gamma = 0.28$, smaller than that of Belle. And this will lead a closer decay point of B mesons and its anti-particle.

2.2.1 Requirements of SVD

The main characteristics of SVD in Belle II matches with the vertex environment quite well. The acceptance angle of SVD covers from $17° \sim 150°$, determined by the radius of PXD($38mm$) and CDC($140mm$). By tracking the trace from outer detectors such as CDC and fitting with the pixels in PXD.

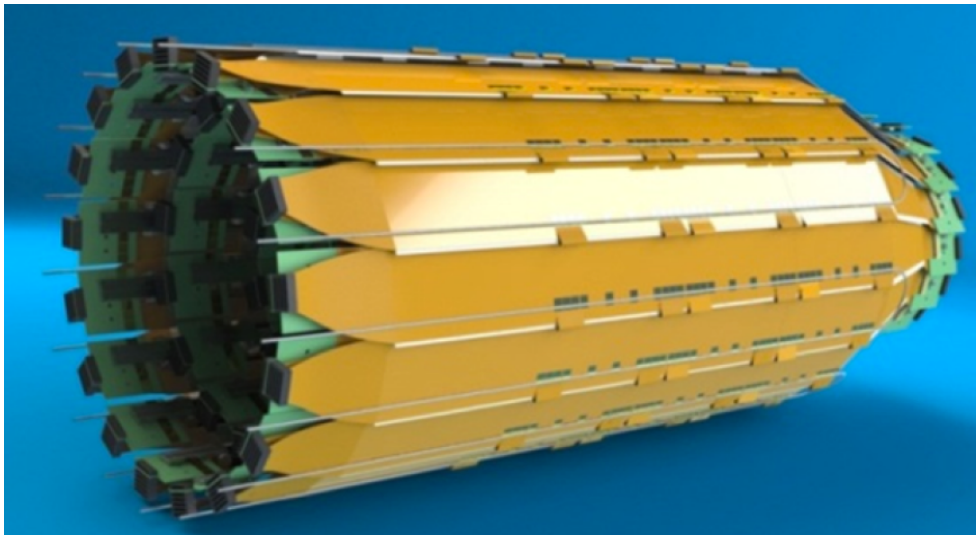

Figure 2-3: SVD structure with two side of hybrids readout and Origami flexible boards.

According to the experience of Belle experience, the high occupancy should be assured lower about 10% in order to get correct associated relationship between tracks reconstructed in CDC and hit combined in vertex detectors. Therefore, the proper two sides signals combination and geometry selection will be of much importance to eliminate combination background like ghost hit in SVD.

SVD must also apply its functions to low transverse momentum particles, such as slow π from D^* decay, which will not hit out in CDC. And it must have also enough reconstruction efficiency for those rather long life particles such as K_S mesons. Since K_S is a very important daughter particle in processes like $B \to K^*\gamma$ and $B \to K_S K_S K_S$ in which the only charged tracks come from π.

SVD's associated software environment robustly maintains peak performance through ongoing and frequent calibrations, alignments, and monitoring.

2.2.2 SVD Layout

SVD is composed of 4 layers of "Double Sided Silicon Detectors" ("DSSD"). The radius of these layers is listed as below:

Layer	Radius	Ladders	Sensors/Ladder	Sensors	RO chips/sensor	RO chips
6	140	17	5	85	10	850
5	115	14	4	56	10	560
4	80	10	3	30	10	300
3	38	8	2	16	12	192

Table 2.4: SVD radius and readout chips numbers(128 channels per chip) , the most inner layer of SVD is indexed as "3" according to the scheme after the numbering of 2 PXD layers.

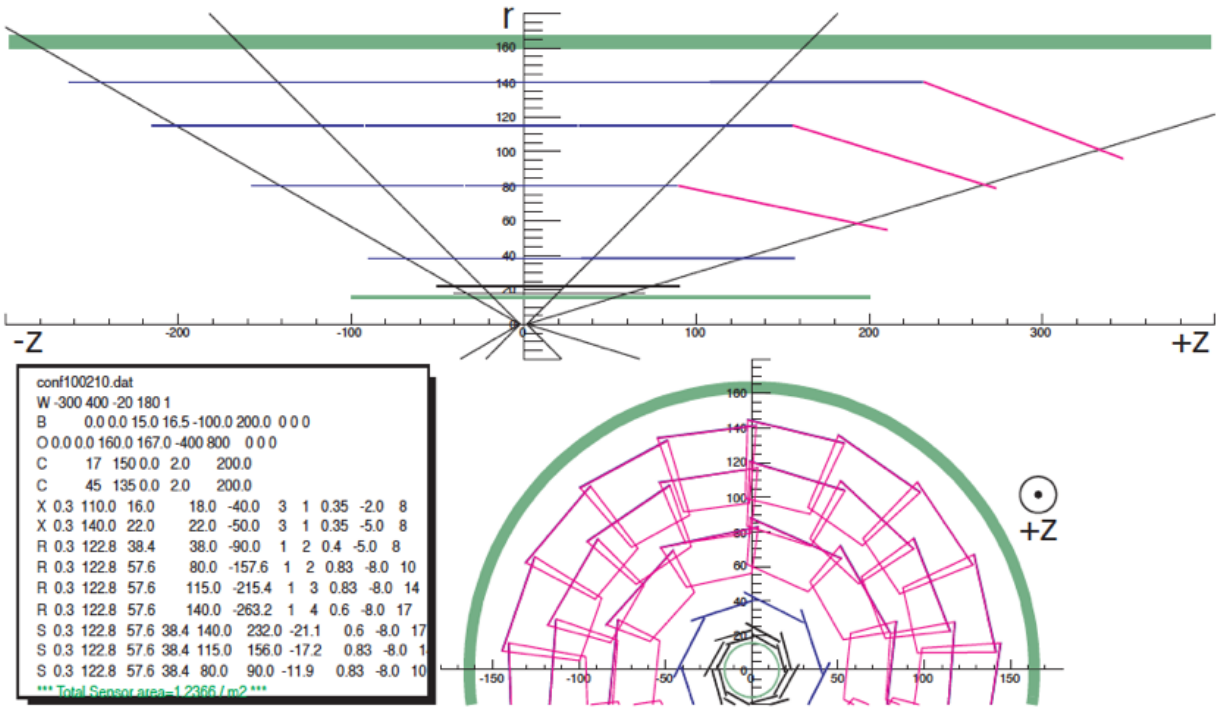

Figure 2-4: All SVD sensors (and PXD) configuration

All DSSDs are located around the beam axis Z and have a small overlapped area on the edges of them. P side of the sensors are parallel to and facing the Z axis. N side is facing towards the outside of detectors. The dimensions of sensors are demonstrated as Fig 2-5 and each of them are connected to APV25 chips.[11] The parameters of the rectangular sensors and trapezoidal sensors are listed, with the floating strips fraction, mechanical parameters and electronic parameters in Appendix Table A.1 to A.4. And the pitch condition for sensors are listed here:

Sensors	rectangular (small)	rectangular (large)	trapezoidal
pitch of P (μm) side	75	50	$50 \sim 75$
pitch of N (μm) side	240	160	240

Table 2.5: pitch distance of floating strips on different shaped sensors

2.2.3 APV25 readout and Origami design

To suppress the background hits, the fast readout chips with shaping time $\mathcal{O}(50ns)$ are highly necessary and they have to be front-end, immune to radiation damage. In 2003, an assessment of readout ASICs was done, and the APV25 [12], which was originally developed for the CMS silicon tracker, was chosen for the future vertex detector readout.

Except for the sensors that are located on the edge of acceptance and the inner layer 3, which are used to be called "conventional FLEX (flexible print circuit) as it was in Belle SVD", all the sensors are covered by the APV25 chips and readout system embedded structure called Origami which means "flexagon" in Japanese. This design is specialized for solving the issues that fast shaping time associated with higher susceptibility to noise. This "Chip-on-sensors" Origami concept helps to solve the issues well. Simply speaking, Origami design locates the APV25 chips on the Origami FLEX on top of sensors with an air-ex layer between them, then the wire bonding operation performs wire bonding from the other side of sensors to the APV25 chips. In assembly of SVD ladders, the position accuracy of wire bonding and the gluing of covers of Origami is the key to the assurance of the quality of whole since the

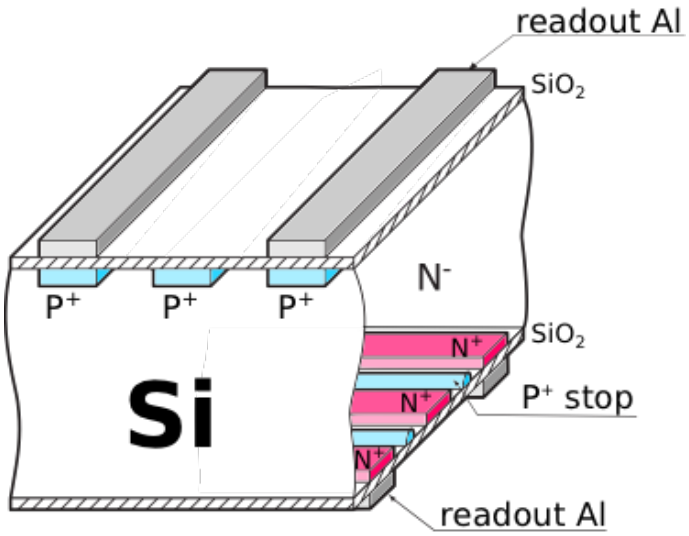

Figure 2-5: DSSD silicon depleted structure

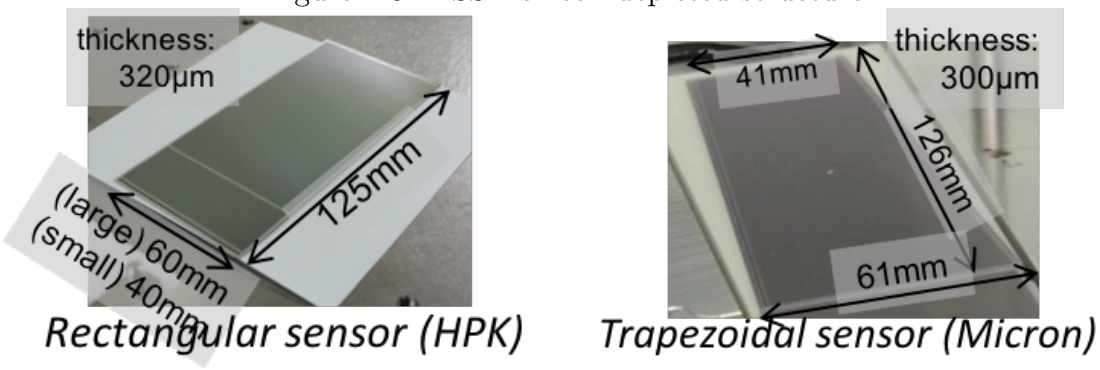

Figure 2-6: Rectangular sensor (left), large (60 mm) and small ones(40 mm) and Trapezoidal sensor (right)

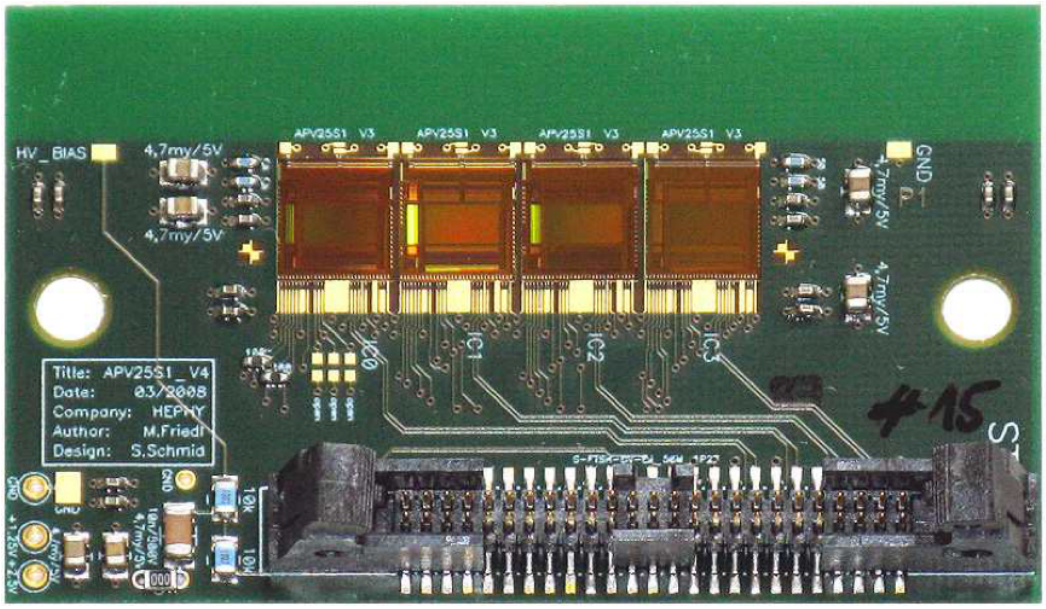

Figure 2-7: APV25 chips on test PCB board

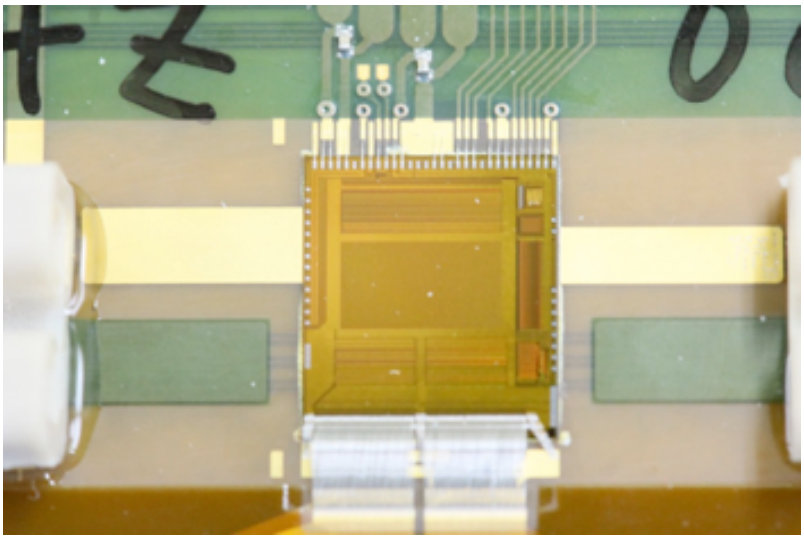

Figure 2-8: Block of one of 128 readout channels of APV25 front-end chip

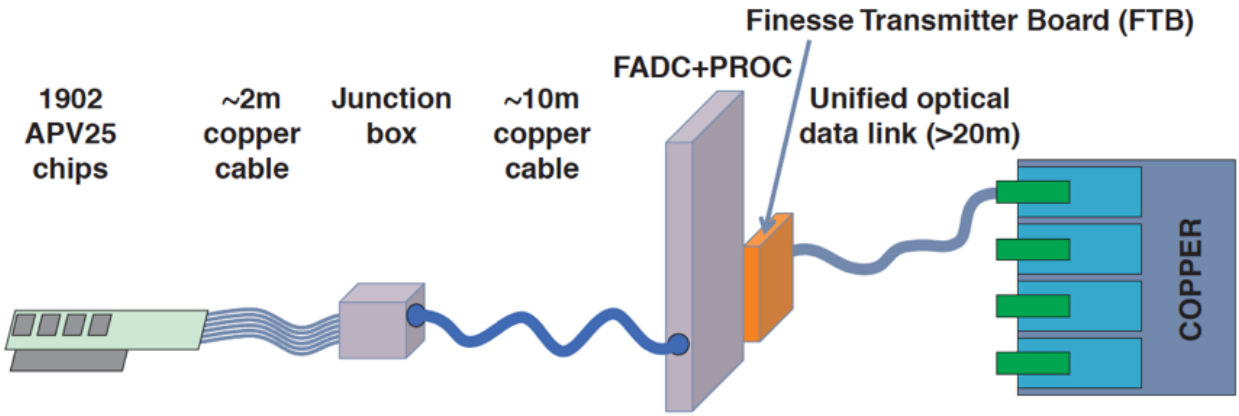

Figure 2-9: Schemetic view of SVD readout chain

mismatch will not only affect the tolerance of ladder under an extreme environment close to IP but also directly affect the readout quality of SVD. If the Origami is not proper wrapped bonding to the APV25 chips, the sensor can not transit any useful signal out and have to be replaced by new one.

2.3 Ghost hits reduction

To meet the vertexing environment of Belle II, SVD has been designed and produced as a set of multi-layers double sided strip detectors. Like we introduced in the section 2.2.1, the occupancy has to be controlled in lower 10% and need to be optimized as low as possible in order to find proper tracks with outer detectors. However, the feature of SuperKEKB creates average 30kHz trigger rate environment and it benefits the physics with a high statistical accuracy, although the overlapping noise and $B^0 - \bar{B}^0$ background become a challenge. This leads a desire to reduce the background through software side, such as finding proper variables to distinguish the physical hit from an interested particle rather a background noisy signal.

Especially in one SVD event, two side of strips read-out channels can cause combined background from wrongly associating two-side hit from two particles or electronic noise into one (see Fig 2-20), and it's named "ghost hits" since they are completely programmed background and has no physics process related to. The work of

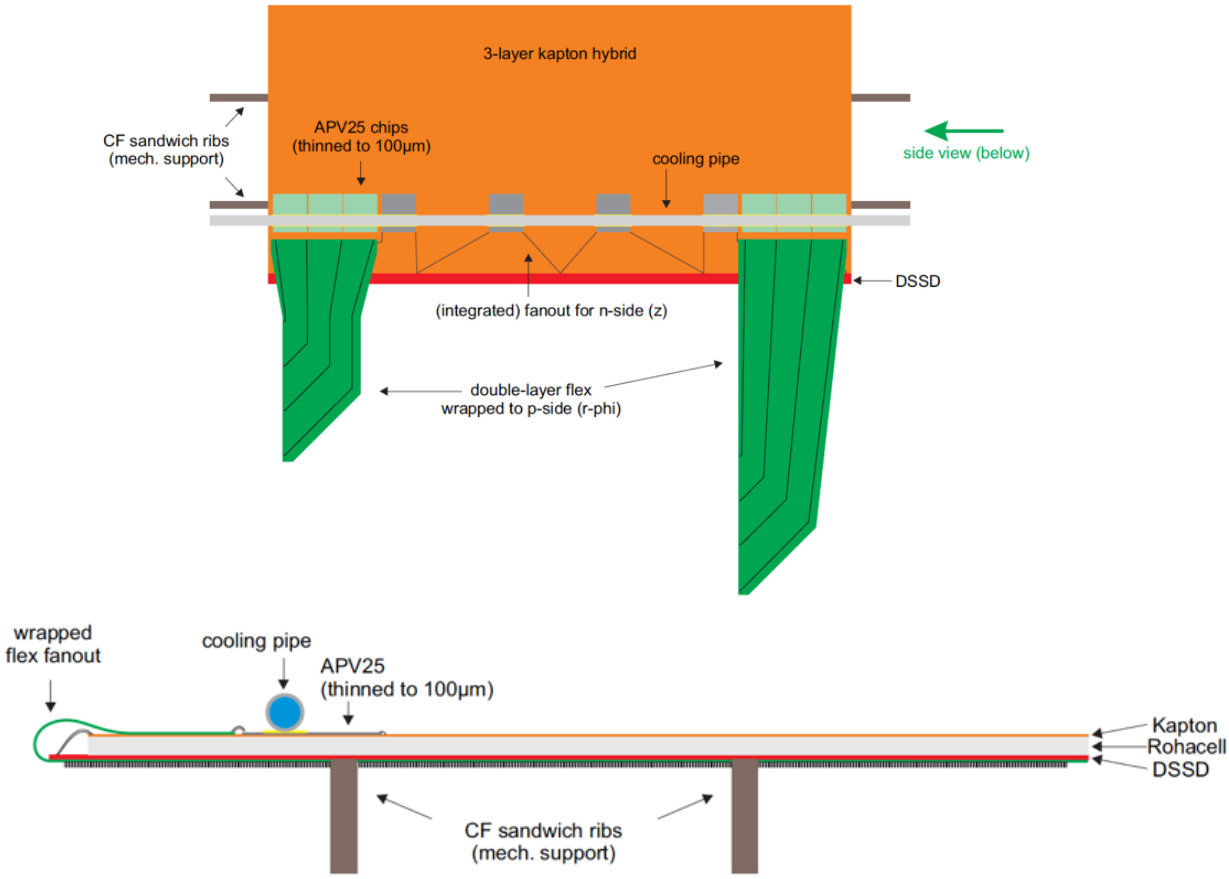

Figure 2-10: Top view and the side view of Origami FLEX with cover(orange) cooling pipe (gray) and wrapping belt (green)

.

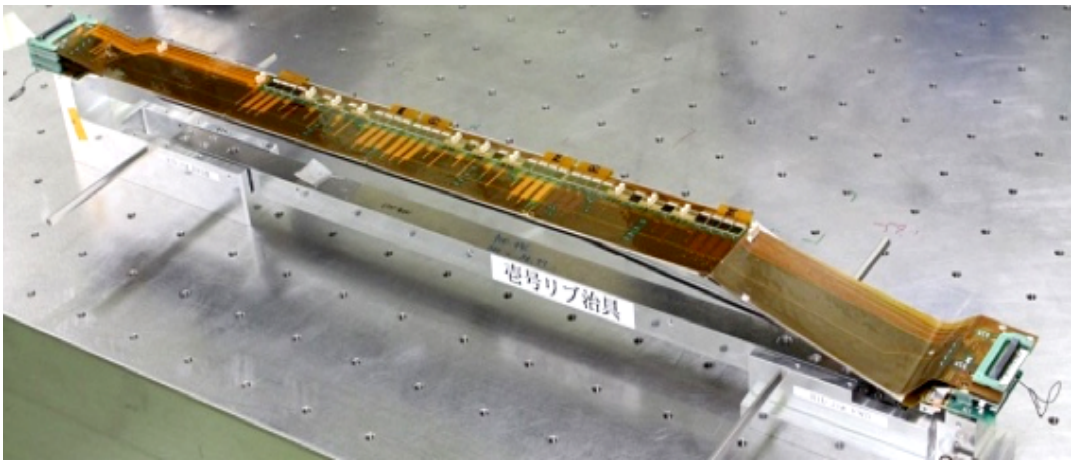

Figure 2-11: Single ladder of SVD on the assembly operating instrument

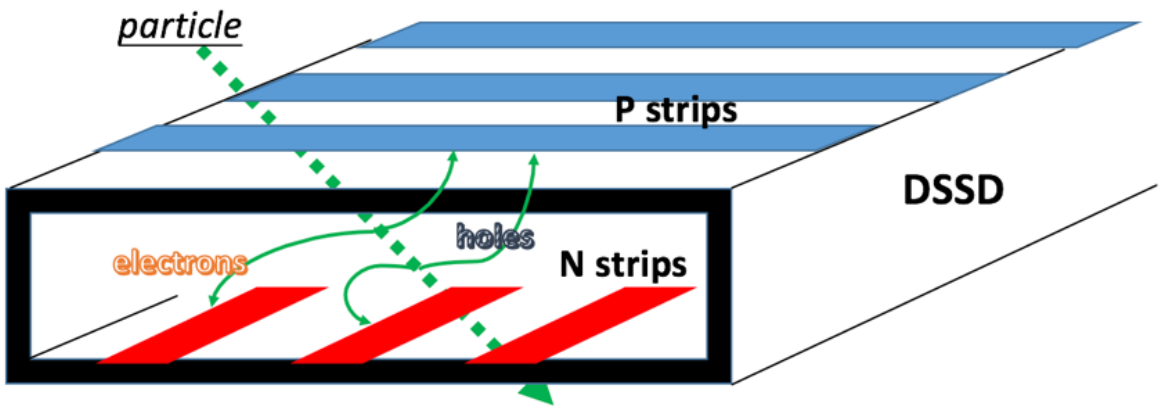

Figure 2-12: illustrative process of particle depositing energy in SVD depleted area and create two side signal correspondingly.

.

tracking can surely eliminate most of these ghost hits since only the ones who close enough to real hits will make trouble to tracking, but still, the rest of them is a concern from Belle experience and simulation. It mainly refers to the occupancy on layer 3 of SVD due to its close location to the interaction region. The event rate can be roughly regarded as inverse-square of the radius which is positively approved by the latest background simulation with Geant4, beam-beam interaction, QED event generator. It should be pointed out that the estimated BG has uncertainties due to the experimental conditions; degree of vacuum, beam optics, simplification of small component in simulation model, and the misalignment of object, nonuniform material in composite object and so on. These will be checked in Phase 2, which is the operational beam test with SuperKEKB and Belle II detectors in the start of 2018 year.

Moreover, tracking in Belle II is based on the hit, which is a spacepoint independent from detectors, input to the data handling path. Tracking is one of the most time consuming process of online data tracking and it is crucial to the high level trigger (HLT) by offering the selection of Region of Interests(ROI) in PXD sensors to cut off useless signals. This raise a need for fast tracking speed and apparently, losing such time on fitting the track where ghost hits locates isn't a wise choice, not mention that there is a limited requirement in data taking speed on readout band-

width for PXD and SVD, see Table 2.5. In general , the High Level Trigger (HLT) will use the selection from fast online tracking to reduce the PXD data readout. Raw PXD data will be stored in buffer called "ONSEN" system for up to 5 second, which means the full event fast online tracking should be kept within this window. SVD online tracking, as a very important part of it, is supposed to be as fast as it can be. Then, the effective ghost hits reduction on software is rather meaningful to save the computational resources, which in general it's where this thesis stands for.

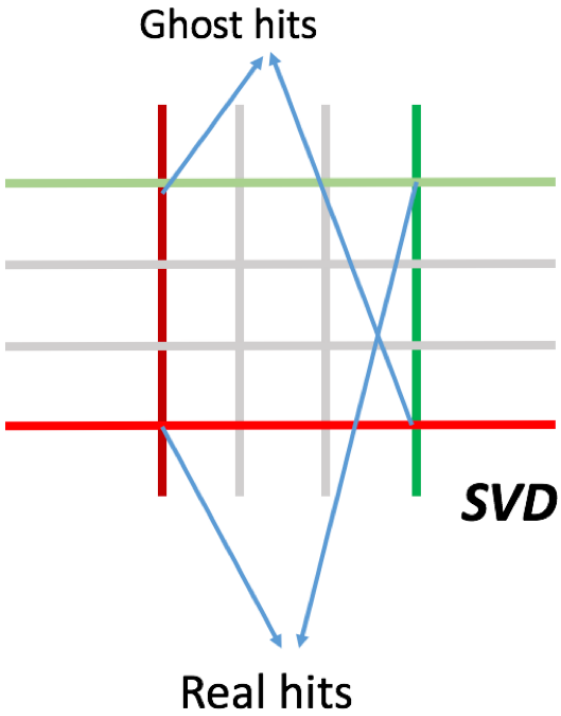

Figure 2-13: illustrative scheme for ghost hits, similar color means readout from a true hit, and wrong combination happens when two or more hits are recorded in one event.

-	#ch	occ	ch size	evt size	total
-	-	%	bit	bit	bit
PXD	8M	1	4	320k	7.2G
SVD	24k	1.9	4	18.5k	555M

Table 2.6: Estimated average occupancy and data size and required number of sub components, ch and occ stands for channel and occupancy respectively.

Driven by this demand, we would like to take other information excluding location of hits into account to reject ghost hits, such as the charge deposition and timing information. Charge deposition from one particle can be regarded similar on both side of SVD sensors rather these from different particles are not, or least not has to be. The potential deviation of charge deposition could be used effectively to distinguish ghost hits. To fulfill this idea and realize the significance of the thesis, a comprehensive understanding of Belle II software structure and function becomes a must particularly in tracking part. Following chapters will start from the introduction Belle II software, leading a way to the realization of ghost hits reduction feasibility study using test beam data sequentially.

Chapter 3

Software for Belle II SVD

As we introduced in the former chapter 2, the success of Belle II experiment put a high emphasis on the success of tracking daughter particles from B meson and vertexing of B meson in VXD, which is directly related to the performance of PXD and SVD tracking ability. Tracking as a core module during the experiment construction is essential. In this chapter, the current tracking strategy in Belle II, especially for VXD, is implemented.

3.1 Belle II Analysis Software Framework

Extracting precise physics results from the obtained data requires large-scale computing capabilities, high-quality software tools and advanced analysis techniques. The full event interpretation (FEI) recovers the information partially and infers strong constraints on the signal candidates by automatically reconstructing the rest of the event in thousands of exclusive decay channels. Belle II Analysis Software Framework II (basf2) is the very fundamentals of all analysis tools developed for Belle II, which gives an set of tool-kits, commands and libraries for exploiting more detailed software functions for all needs such as data taking, event building, tracking and so on.

Just as the upgrade of SuperKEKB from KEKB and Belle II from Belle, basf2 is the software framework that is rewritten and redesigned for a better usability and analysis friendly user experience, higher stability and code quality respect to

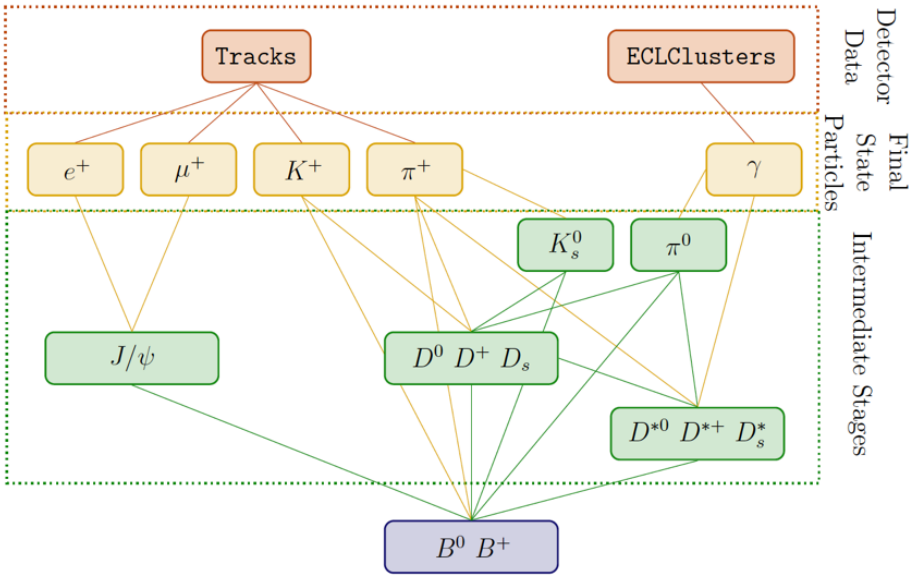

Figure 3-1: Hierarchical approach of the FEI

.

its predecessor basf1. It has been designed to keep a high consistency of analysis procedures on online and offline data handling. The framework is written in C++ for most of data storage classes and modules definitions as well as Python for flow control and specific analysis tools. In addition, it supports the many popular third party functions by introducing libraries such as EvtGen, ROOT and Geant4. The visual structure of basf2 is demonstrated as Fig 3-1.

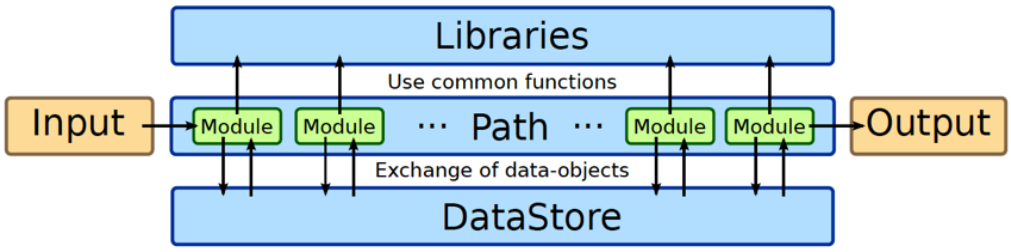

Figure 3-2: Modules perform data analysis on each event in a data input using the functions provided by libraries and information embedded in objects called DataStore.

3.1.1 Basf2 architecture

The basf2 framework works based on many Modules chained to a path normally called "main". These modules are stored in packages, divied by their functionality on different aspects of data handling. Generally speaking, they can be itemized as:

- Data acquisition (DAQ)
- Event generation (EvtGen)
- Geometry of general detectors
- Sub detector simulation (PXD, SVD, CDC, etc...)
- Tracking and reconstruction (VXDTF...)
- Visualization of individual events inside the detector (display)
- Physics analysis

Packages contains Modules, libraries and data objects. Modules are basic analysis blocks of functions in a chain of them called 'path'. The job of each module is to handle the data from data objects, using the functions from libraries, modifying, adding or deleting some structure of data object in a duration of one event, then passing the data object to the next module which is registered in the same path.

Data objects are store in a framework object called DataStore, writable and readable for all modules. Here come a few examples of data objects such as "Track", "SVDClusters", and "Particle". But since the physics process constrains that in one event, dataobjects are built based on some specific orders and relations, so data store also restore the relationship between these variables, like a "SVDClusters" have a relationship with a "Track" by a pointer indicating the index of it in this track. And building the relations of data object is also important to maintain the persistence and providing interface for multi-tasking processing, distributing computation and real time monitoring.

Basf2 conducts data handling through a steering files in Python that tells the sequence and what functions basf2 needs to do. In the steering file the path is created and filled with modules, afterwards the path is processed. Input and output data files can be read and written by adding the RootInput and RootOutput modules at the beginning and end of the path, respectively. The input and output data file names can be either passed to these modules as arguments or specified via command line arguments. One has to distinguish between two levels of code execution. Firstly, the Python steering file is executed and builds the path (steering level). Secondly, the path is applied to all specified events (path level), usually the code executed at this level is written in C++.

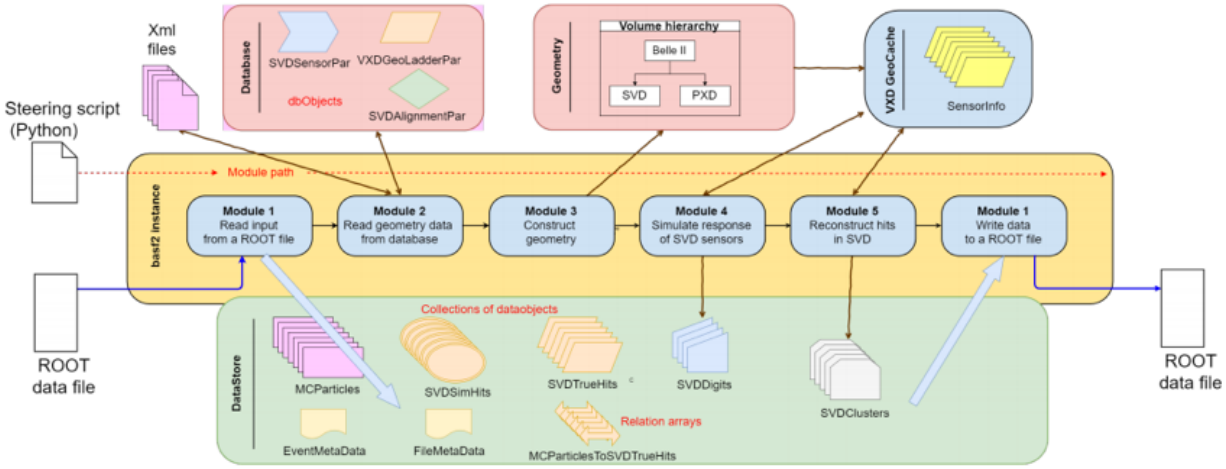

Figure 3-3: Basf2 simulated data flow of SVD events.

3.1.2 Online tracking and HLT

The High Level Trigger (HLT) in VXD level seizes the information from PXD and SVD readout to determine if one event is a true physics process that is worthy of being recorded and built as a event. When VXD works, tons of hits will be recorded in PXD and lesser mount of clusters will be readout on SVD sensors. According to section 2.3, one has to distinguish the physics hit from vast background when building event. So fast tracking is needed for SVD hits to get tracks, then fitting with SVD tracks to

extrapolate their incidence on PXD panel, determining the region of interests (ROI). After the HLT, only a small region of hits on PXD will be send to the event builder to be recorded to offline data set, since the high luminosity creates an average 30 kHz rate and the data buffer is limited, the performance of HLT can be essential of good data taking in software. [13] A data acquisition system for the silicon pixel

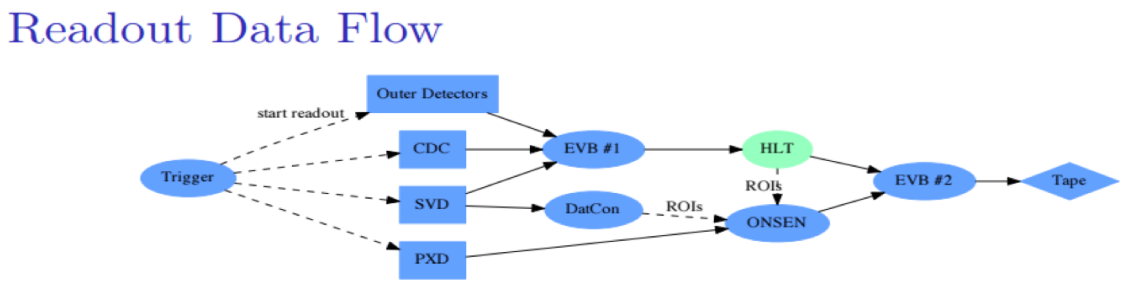

Figure 3-4: Two step event builder in Belle II, firstly data from SVD and outer enters the first event builder and tracking&fitting to generate HLT information, then HLT will intercept ROIs on PXD panels to reduce data, event builder 2 will only store the HLT information and ROIs on tape for offline.

detector called "ONSEN". The occupancy of the pixel detector is estimated at 3%. This corresponds to a data output rate of more than 20 GB/s after zero suppression, dominated by background. The Online Selection Nodes (ONSEN) system aims to reduce the background data by a factor of 30. The ONSEN system buffers the entire output data from the pixel detector for up to 5 seconds. During this time, the Belle II high-level trigger PC farm performs an online event reconstruction, using data from the other Belle II sub-detectors. It extrapolates reconstructed tracks to the layers of the pixel detector and defines regions of interest around the intercepts. Based on this information, the ONSEN system discards all pixels not inside a region of interest before sending the remaining hits to the event builder2. [14]

Currently, there is no combined experiment of VXD and CDC so CDC hits will not provide anything to HLT yet. Considered that the purpose of online tracking draws a special need for reducing PXD data merged into offline, the work of HLT requires a fast data processing in online tracking, then it has to meet the requirements as following:

- Data reading of VXD format

- efficient track finding and fitting

- extrapolation of tracks to PXD planes

- definition of ROIs

- successful communication of ROIs to the ONSEN systems

Common configuration data such as the description of VXD geometry is stored in XML files which are varied based on the simulations settings and test beam or real experiment. The software employed on the HLT is the same software as is used for offline reconstruction. Indeed, all software used during the testbeam were the then-current versions of the software for the Belle II experiment.

3.2 Offline tracking

In HLT construction, one can find the importance of tracking playing a key role in the analysis path, and since the EVB#2 in Fig 3-4 will combine data from HLT and PXD ROIs from ONSEN into a completed set of data on tape, those information will also be avaible for our analysis when retrieving the information from beam test data. Both online and offline tracking mainly works through tracking package offering module called "track finder", more specifically for our interest, is track finder in VXD (VXDTF). When introducing tracking, the detailed principles of HLT generation will also be explained since it needs track finder to give tracks for ROIs determination. And for future offline physics analysis, tracking packages will provide basically same functions as they do here.

First of all, the core of tracking package is GenFit, which is widely used as a basic toolkit of track fitting by many experiments in the world, with a good extension to the individualized features[15]. It gives us three modular components: track representation, track hits from detectors and fitter, to build up our own code. The performance of tracking is high dependent on simulation result input, because simulation will give

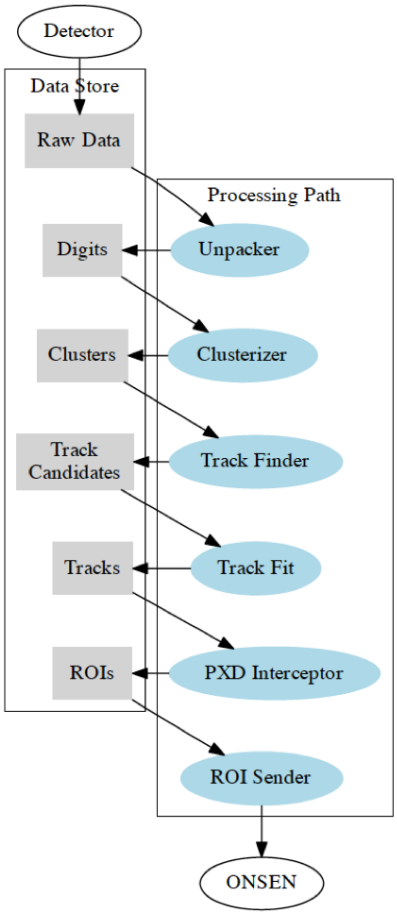

Figure 3-5: Block diagrams of data flow in Belle II HLT process. Blue ones are modules that performs the processing and grey ones are data store.

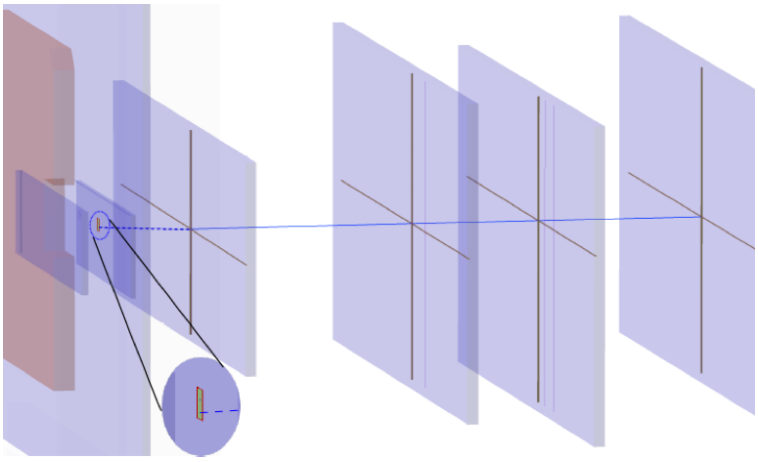

Figure 3-6: Track fitter will fit the track from a list of hits and extrapolate it into plane of PXD for ROIs (small green part),The size of the array is determined by both the extrapolation errors and an allowance for systematic errors such as misalignment

tracking modules information about the patterns of a particle's interaction with one detector, and hit classes rely on simulated input as well.

When detector hits are loaded for tracking, the pattern recognition will give candidates of possible hits to GenFit. If doing a simulation, the MC particles will be convert into detector responses by Geant4. These clusters class based data are shown in Fig 3-5 as "clusters" block. Then TrackFinder will collect necessary hits to form lists of hits to create TrackCandidates (TC) to fit with fitter, such GenFit2 package. The output of this step will generate the smoothly fitted version of TC - Tracks, or other Track level class like RecoTrack which store not only the hits information but also access to fitting results, such as momentum, energy,etc. See the last step of blocks in Fig 3-5.

3.2.1 Modules and definitions

When one uses data from experiment, the responses from detectors are all collected by online data taking. But since the setup of experiment and beam tests can be varied then the simulation has to be flexible and extendable to fit in different situation, which requires corresponding software's configuration being adapted. In simulation, the corresponding modules are particle gun, Gearbox, Geometry, which will be discussed in next section.

The whole data flow after the signal taking can be depicted majorly as Clusterizing $\rightarrow$ Reconstruction $\rightarrow$ Track fitting, like you can see in Fig 3-5. Main modules and packages are listed and explained as following:

- **PXD and SVD Unpacker**;

  These are modules that release the raw format data into PXD or SVD digits, which are pixel or strip level signals from APV25 chips.

- PXD or SVD Digitizer;

  Aftering getting digits data of VXD, digitizer can transfer the electrical signal into the physics information such as charge deposition.

- **PXD and SVD Clusterizer**;

  The strip level signals need to be clusterized since when particles penetrate silicon sensors, the energy deposition are diffused into multiple pixels or strips. It gives PXDClusters and SVDClusters along with their attributes as output, which is the most important variables because they are fundamental variables that have actual physics meaning and easy to handle, representing the interaction patterns of particles and sensors. They are also the input for VXDTF to find tracks.

- **Reconstruction Packages**;

  There are quite a few modules in reconstruction packages such as Gearbox, Geometry and VXDTF. Each of them provides the information or algorithm to do reconstruction that is basically a process of collecting hits on SVD layers to give out clean TCs. The detail of VXDTF will be implemented in following sections.

- **GenFit for track fitting**;

  Like mentioned in early section, TCs will be converted to fitted Tracks.

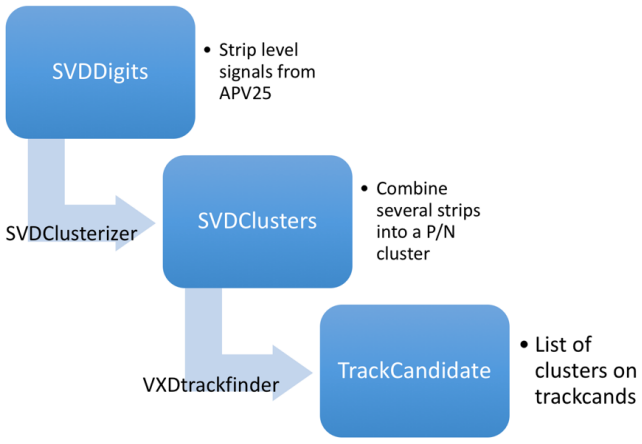

Figure 3-7: Main work flow of reconstruction

3.2.2 Simulation of SVD

From the introduction of basf2, the run information and event information can be addressed through the given modules 'EventInfoSetter' in a steering files about how many events or runs that you want to do. In common cases, simulation of VXD consists of two parts to output data: particle generation and interaction simulation. The former one is the done by EvtGen and later one is done by Geant4. Specifically, the signal particle generation plays it role by Module called particle gun using libraries in EvtGen, which basically gives out particles in a range of energy and momentum. The interactions of particles then can be simulated in Geant4 in a way that allows users can configure and customize the simulation parameters easily in code.

Geant4 tracks provide information about passing particles and energy they deposit in the SVD. This energy is used to calculate the amount of electron-hole pairs generated along the track of the particle. Electrons and holes are driven to the readout strips inside SVD sensors, and under many cases these pairs will be absorbed by over one strips due to the incident angle and diffusion of charges. One thing need to be clarified is that not all the strips on SVD sensors are bond to readout band of APV25 chips, simply to reduce the readout channels from a huge mount of strips to limited APV25 chips per sensor, see section 2.2.3 and Tab 2.4.

For those strips (we call tem floating strips) who are not connected to APV25 chips, signals are coupled through capacitance between readout strips, demonstrated as Fig 3-9:

This will lead the redistribution of charges among the neighbouring strips even through floating strips accumulate charge in the same way as readout channels, see Fig 3-8 and Fig 3-9. The electron-holes pairs will be generated by Geant4 simulated energy loss, then drift and diffusion of electron-hole pairs will be calculated and absorbed by nearest strips, Fig 3-10. This is more than just an effect worthy of noticing, as a matter of fact, since the shape of the sensors of SVD are not always rectangular but trapezoid and distributed capacitance is affected by pitch, then actually capacitance used in simulation is a troublesome issue, which requires careful handling and

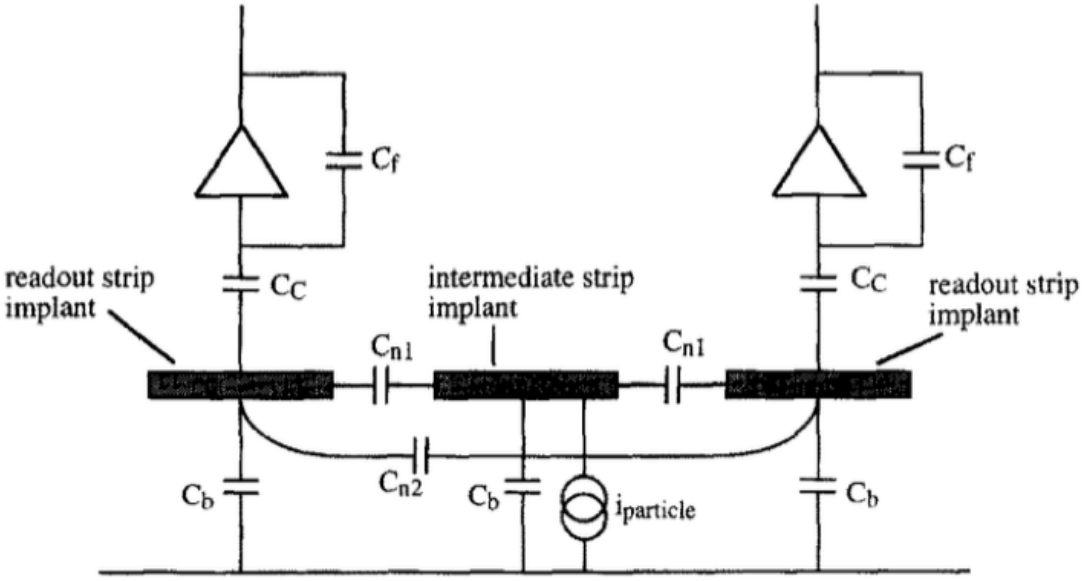

Figure 3-8: Floating strips couple their signals through capacitances to readout channels

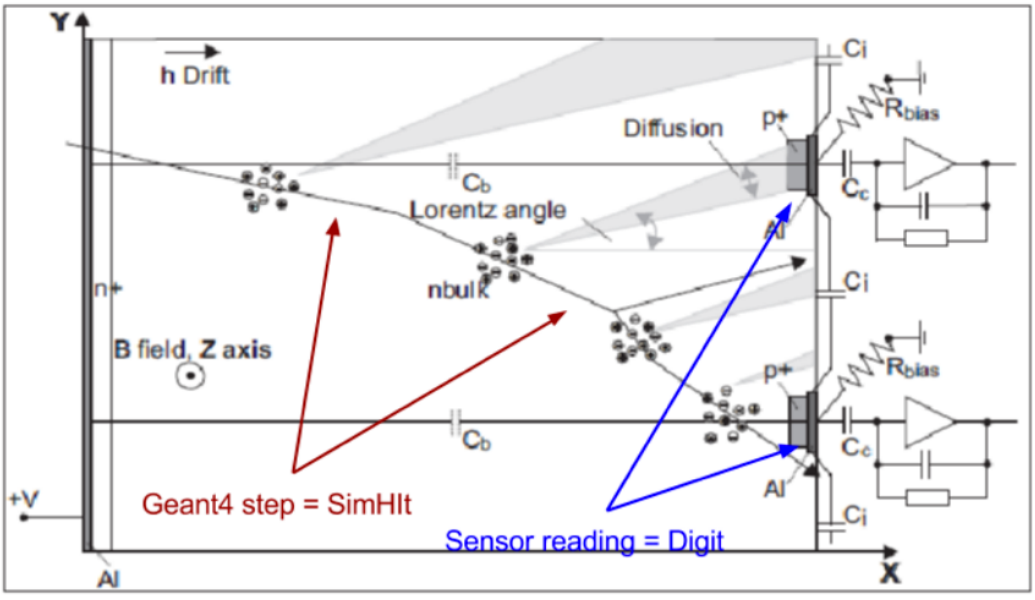

Figure 3-9: Energy deposition process and floating channels structure.

calibration. Otherwise, the output signal amplitude will be totally false resulting MC validation of VXD related analysis impossible. This issue will be addressed again in our analysis result and offline calibration solution will be given from our study as well considered that real measurement of these capacitance on sensors may not be realistic. And the parameters of sensors are varied from sensors type, and I put the basic and electrical parameters charts in Appendix A.

$$S_i = \sigma \sum_{k=-2}^{2} \sigma_{|k|} S_{i+k} \tag{3.1}$$

$$\sigma = \frac{C_c}{2C_i + C_b + C_c} \tag{3.2}$$

$$\sigma_0 = 1 \tag{3.3}$$

$$\sigma_1 = \frac{C_i}{2C_i + C_b} \tag{3.4}$$

$$\sigma_2 = \frac{0.5C_i}{2C_i + C_b + C_c} \tag{3.5}$$

C_c is coupling capacitance, C_b is back plane capacitance and C_i inter strip capacitance.

Simulation of energy deposition and physics-to-electronics is done mainly by SVD-Digitizer as introduced in section 3.2.1. After couple of years update, the performance of SVDDigitizer has beem approved fairly stable in the last two time beam test and simulation. From the recently discovery of issues of floating strips capacitance, SVD-Digitizer is what needs to be taken care of. We have found that the description of capacitances in SVDDigitiers are wrongly valued and require further calibration in offline. By scanning the parameters in SVDDigitizer who defines values of capacitance, simulation of SVD charge deposition of multiple strips signals could be aligned and calibrated to keep persistence with experimental data such as beam test.

3.2.3 Hit Reconstruction

Clustering is the first step to build up SVD event. According to Fig 3-7, the digit data from SVD will be set into bunch through SVDClusterizer. The clustering in PXD

panel is 2D so that we do expect the similar output for SVD, which we clustering on P and N side respectively. The threshold set for clustering is as recommended to be 3σ in amplitude distribution adjacently. The input for clustering is the digitized charge deposition represented by amplitude of signals and timing on each strip. When only one strip passes the threshold, the position of clusters is identified on it, while multiple strips form a cluster, the Center of Charge Gravity (CoG).

This may lead two error systematically on **hit reconstruction**, the first is unseen-charge-based position error. When adjacent strips signals being ignored, the true position of the cluster is off aligned. Other one is, when adjacent strips also pass the threshold to give out signals, CoG method only gives position based on charge sharing on these strips instead of the real middle point of projectiles inside the sensors.

Once the hit reconstruction is finish, which means signals from SVD form a set of clusters on each layer and side, VXDTF can load data to perform tracking. In order to cope with the algorithm, clusters unit data will be reloaded as a couple of classes like RecoHits for directly usage of VXDTF and spacepoint (SP, P cluster+N cluster). Specifically how VXDTF works is described next and it's crucial to our results.

3.2.4 VXDTF

Again, as discussed in section 3.2.1, VXDTF does critical work in the chain of reconstruction, and its algorithm is based on sector map concept. Motivated by doing fast filtering for reducing possible hit combinations until more complicated filters can do the finishing, a step-wise look-up table for fast selections of hits must be used. To do that, we create a concept called 'sector map', which pre-defines some position cuts for hits used in VXDTF. Before the loading of hits from sub-detectors like SVD, VXDTF will use the pre-configured geometric map to sort the panels of SVD layers into smaller pieces of sector map that are all rectangular shape. Then SVD clusters from two sides, will be added into 'SpacePointCreator' to combine a spacepoint (SP) when the selections of SP approves them to do so [1]. At this moment, the SPs will

[1]By default, SP creator will simply combine all the input SVD clusters, which is where this study tries to help, adding selections to SP for rejecting ghost hits reduction.

be divided and addressed into different sectors settled before in sector map, then VXDTF will generate segments by connecting two sectors that are 'friends sectors'.

Here, 'friends sectors' are stored in sector map, and specific cuts of hits in sectors can be applied. For instance, one can set a cut to limit the distance between two hits in two sectors, only for these who pass the cut can be used later. Usually, the selections of 'friend sectors' are trained using MC sample, such as one track passing through two sectors on consecutive layers. When the compatible hits that pass the cut are stored, the unit of hits pair named 'cell' is connected, see Fig 3-12.

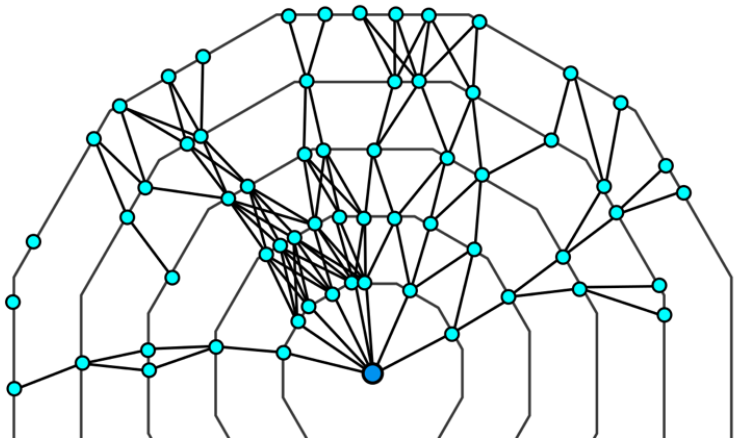

Figure 3-10: cells of all hits pair who pass the cut in friend sectors, constraint by a distance threshold.

Here, cellular automaton (CA), "a discrete dynamical system whose behavior is completely specified in terms of a local relation", is utilized for pattern recognition[16]. Below Fig 3-13 shows the possible TCs which have cells in growing order of values.

For examples, we can set rules 1∼4 as following [17],

1. Two cells are called connected if they share a hit.

2. If two connected cells have the same state and fulfill some criteria qualifying them as possible part of a common track, they are called neighbors. (A possible simple criterion is e.g. the angle between the two segments.)

3. Every cell that has at least one neighbor on the inside raises its state by one at the end of the current step.

4. The steps are repeated until no cell changes its state anymore.

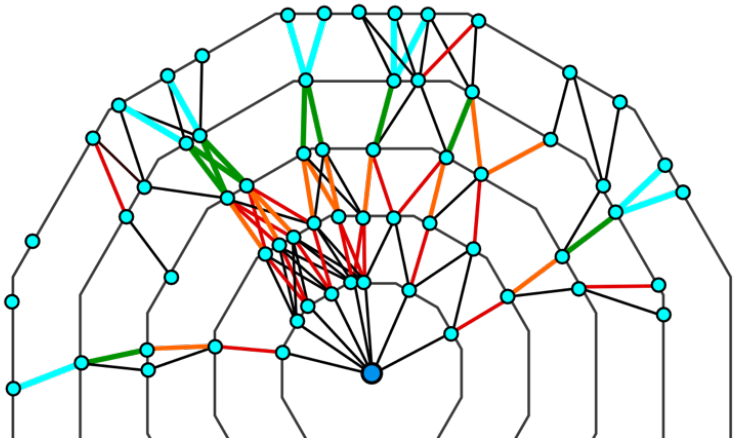

Figure 3-11: CA after 4 iterations,the cells have now different states,color-coded and growing in thickness: 0 (black), 1 (red), 2 (orange), 3 (green), and 4 (cyan)

After the CA, later filtering can add more rules like that every TC shall have more than 2 hits so the number of TCs can be further reduced.

Kalmen Filter (KF) or Circle fit will be used when CA is done, to check the quality of TCs set, also many options of filters can be used. In some situation, the some of TCs we have here still contain shared hits, especially when there are two close addressed hits or ghosts in the same sectors. A neural network of Hopfield type is employed to find a clean set of TCs which there is now overlapping TCs.

When this process is finished under one specific sector map, more rounds can be processed based on different sector maps corresponding to the different range of momentum of tracks. By doing that, even a low transverse momentum p_T TC can be spotted. Here is the schematic flow of track finder in SVD. The overall scheme of VXDTF can summarized as below:

After all, the TCs are uniquely meaningful in my analysis. In data store, TCs are represented by class TrackCands which has attributes indicating its associated hits on each layers. A clean, well filtered set of TCs guarantee the reliability of our data source — hits on tracks. Since the study is focusing on retrieving hit charges from those who are associated with reconstructed tracks, the procedure we would follow is first to get good TCs or its related classes from reconstruction by applying some

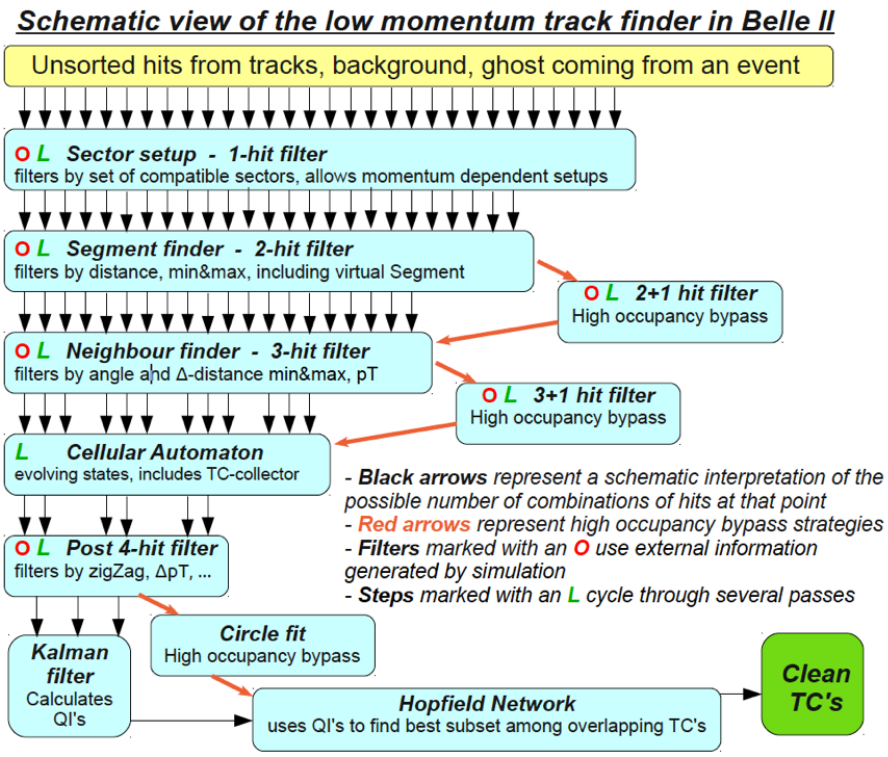

Figure 3-12: Schematic flow of track finder in SVD

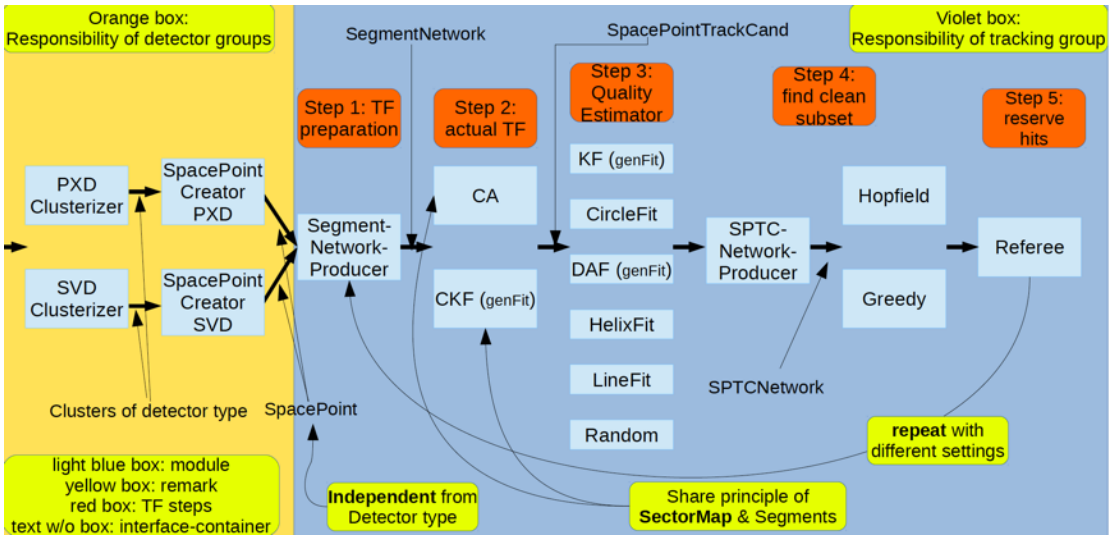

Figure 3-13: VXDTF overall structure

selection rules, made by DESY beam test characteristics, then we can look into some interesting measurement.

Chapter 4

DESY beam test

Before the official run, many early measurements and tests are already scheduled in different stages of Belle II overall commissioning. However, the true quality of experiment in every tiny aspects can only be determined when all the components are settled right and all software are well-prepared, as they are designed for Belle II. It's also required that the SuperKEKB upgrade is finished and tested matching with designed performance. So due to the mismatch of proceedings of all subgroups and collider group, tests of sub-detectors have to started in alternative ways in different timing to keep an eye on the quality of them. Meanwhile, it's helpful to testify the quality of software as well.

KEK and DESY, Deutsches Elektronen-Synchrotron, have a long history in co-operation, in particular in the field of particle physics, where both institutes look back on roughly 40 years of cooperation. DESY has a beam environment at around 2∼6 GeV with adaptable event rate and magnet field setup, which reaches a close energy as Belle II will experience in future, which makes it a ideal one for testing the basic performance of VXD and gathering valuable data about its performance. Since 2013, DESY beam test has been run during different stage of SVD assembly, and particularly in 2016 and 2017, SVD successfully produced class B ladders which were believed to have almost as same quality on electronics as class A ladder for offical mount in Belle II. Results of relative topics from 2016 and 2017 DESY beam test can be regarded as quite instructive and persuasive, helping us understand the truth of

hardware and software.

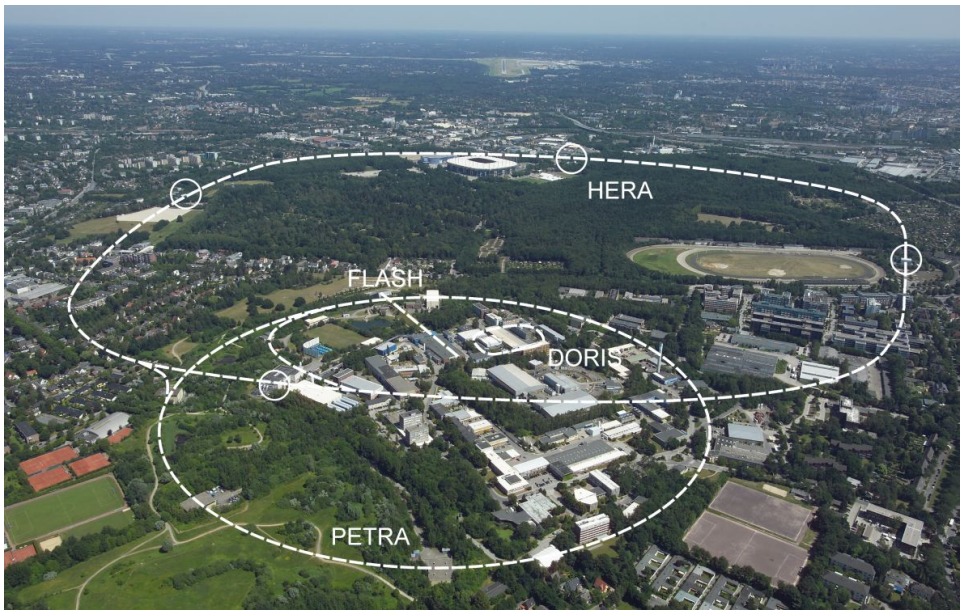

Figure 4-1: DESY bird view sightseeing

As for my topic concerns, the data collected from 2016 and 2017 are both obtained, with same ladder but different beam environment setup, meanly in cooling system installed only in 2017 test. Of course, environments such as magnets and rotation of detectors are not completed same but can be found correspondingly similar in all runs.

4.1 Beam test overall setup

4.1.1 VXD Installation

The first need testing is the VXD integration including environmental monitoring, slow control, full readout chain, HLT tracking and ROI, etc. On software, basf2 functionality is also tested from simulation to analysis. After the installation of PXD and SVD to beam line, combined test can be started, which is the first time test with PXD sensors. The range of beam energy is up to 6 GeV from 2 GeV, and event rate reaches the peak at 5kHz when energy is around 2 GeV. A constant

magnet field at 1 GeV is optionally applied to the direction perpendicular to the beam line direction, bending the beam. To provide supervision and trigger to DAQ system, two extra set of detector layers called telescope, are paralleled placed forward and backward VXD. Each of them are squared $20\mu m$ shape EUDET pixel detectors. All information of DESY beam test including each run setup, environment varibles, purposes.

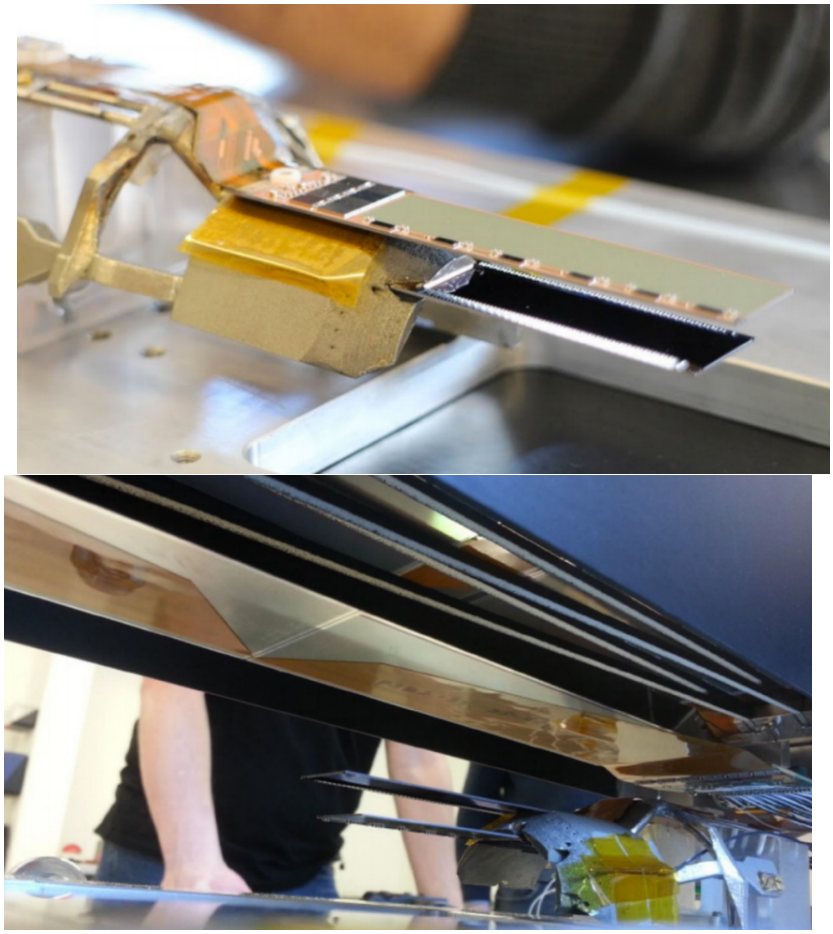

Figure 4-2: PXD sensors in beam test and its position in ladder

4.1.2 Geometry and Setup

Full ladder or half ladder of PXD, plus 4 full layers of class B SVD, form VXD geometry in beam test. Cooling system, installed by using CO_2 as material in pipe attached to the surface of layers. To be noticed, cooling can affect the temperature of

working sensors in the way by reducing the hot noise in depleted area of silicon so that the diffusion and reabsorbing of charge-lets are reduced. Then forward and backward telescope arms are installed. Beam test will firstly penetrate forward telescope

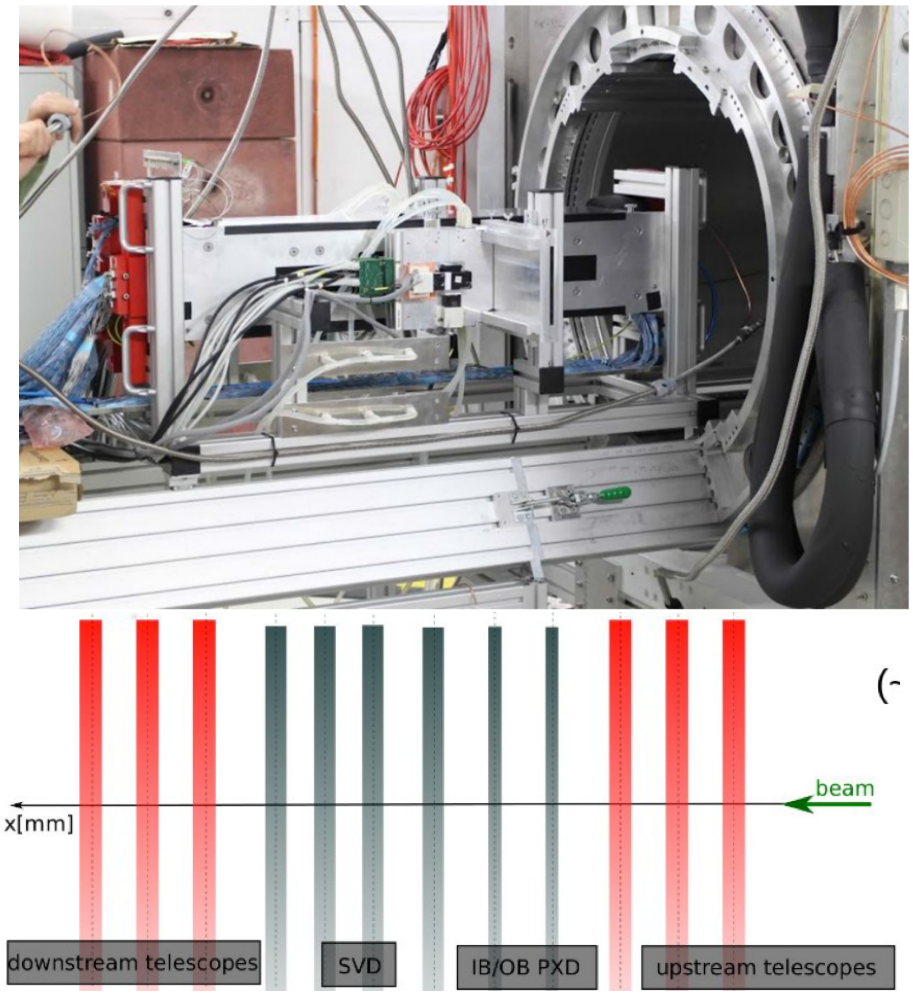

Figure 4-3: Beam test hardware and geometry

layers and the PXD and SVD layers, 6 in total then hit backward telescope. A delayed readout from two part of telescope form primary trigger to record data. In beam test 2016, all runs are conducted with 90° as Fig 4-3 shows, and in 2017 tests, several runs are finished in cases that plane of sensors are rotated with 5,10,15...degrees respectively. Besides the angle, magnet field is set with 1T or none for each runs. Some of the runs are tested under a scan of magnet field from 0 to 1T. Geometry regarding the strip numbering and direction indexing are fundamental to understand

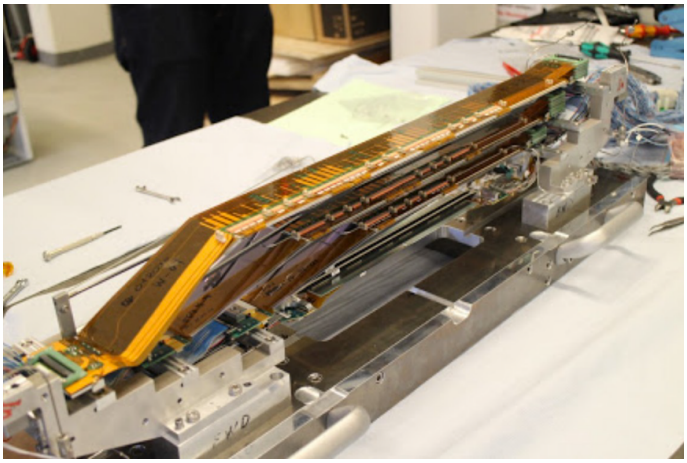

Figure 4-4: Tested VXD layers (PXD and SVD)

the data collection. For instance, in data output, P and N side of SVD are respectively marked by U and V standing for their directions, and their numbering scheme is that on every sensors, from 0 to maximum (767 or 511) vertically to the U or V directions. On each layer, sensors are indexed from 0 to 1 for PXD and 0 to 4 for SVD, forward to backward. Beam directions is set to be W, all as Fig 4-5 shows.

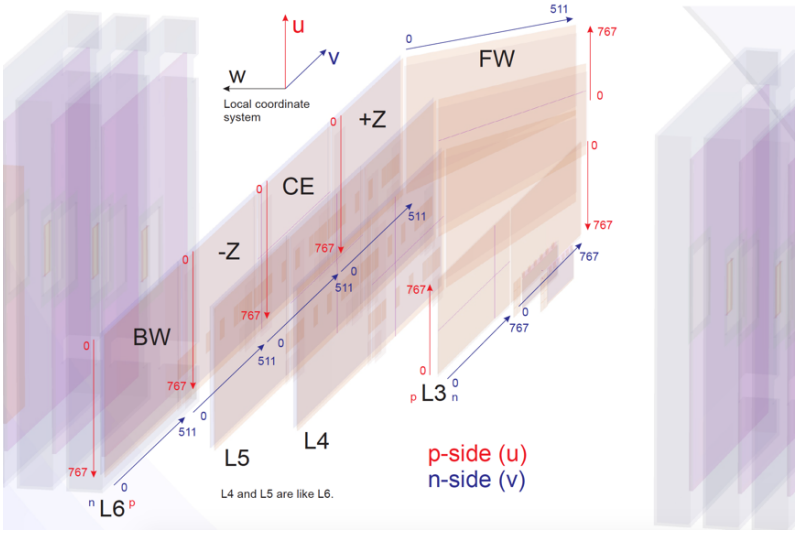

Figure 4-5: VXD geometry scheme with numbering and indexing in local coordinate

4.2 DAQ and HLT in beam test

In terms of DAQ and HLT tracking, the introduction has been made in Chapter3. Full version of DAQ and HLT tracking would be possibly optimized in the future test with some minor changes, but the whole framework and algorithm shall remain much close, and of course, are applied to beam test, with some scale-down. Schematic view of global DAQ of Belle II is put in Appendix B.

The reason for scale-down DAQ is rather simple ,that is in beam test, no CDC component for full online tracking in HLT, so HLT will only be build upon SVD data. As already demonstrated before, HLT uses SVD fast tracking to send ROIs to ONSEN system compared with DATCON. The selected ROIs on PXD will merge the data with SVD data to EVB#2, then for monitoring the fast tracking and ROIs selection, Belle II event display is also implemented. ROI determination using TB events shows as Appendix B-2.

In case that the geometry of beam test and real experiment is different, a specialized package called testbeam is added to the basf2 git repository. This package contains test beam geometry definitions, field map of DESY environment, telescope descriptions and one-ladder sector map for tracking. In VXDTF section, we introduced the sector map concept and how it works in tracking and reconstruction. One must realizes that hardware setup is determinate towards the sector map. When facing the data from full version of Belle II VXD with round covering ladders, tracking algorithm can scan all sectors among all sensors instead of only one ladder to find friends. One ladder can only cover a small range of acceptance angle, and since test beam is mainly 90° to the sensor panels, it may cause hits missing on outer layers. To avoid that original tracking filtering too many tracks in such case, secondary filters after CA processing is re-defined for test beam data to allow partially reconstructed tracks stay in TCs set, because in offline data we care more about the true hits on inner layer 3 rather than outer ones for ghost hits study.

Alignment is specially of importance for data handling. Basf2 provides an integrated full VXD alignment and it's designed to be quite flexible to fit in different test

regarding VXD. So for beam test, only a special configuration is needed in basf2.

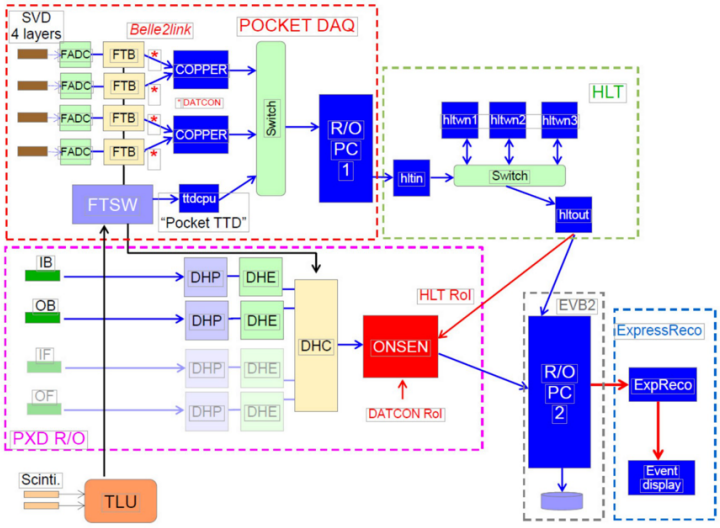

Figure 4-6: DAQ system work flow scheme in beam test

For the purpose of quality check of VXD hardware in beam test, another

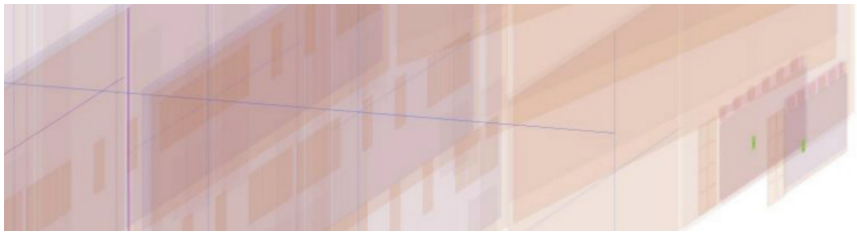

Figure 4-7: Belle II event display function in basf2, green area is ROI on PXD

featured package called DQM (Data Quality Measurement) is included in test beam branch of basf2. DQM can help find the problematic pixels or strips in VXD and put a mask on them so overlook them. It has been known that both PXD and SVD show a stable performance during the beam test and DAQ system runs with expected quality, which only tens of pixels and some edge located strips are much masked and noisy.

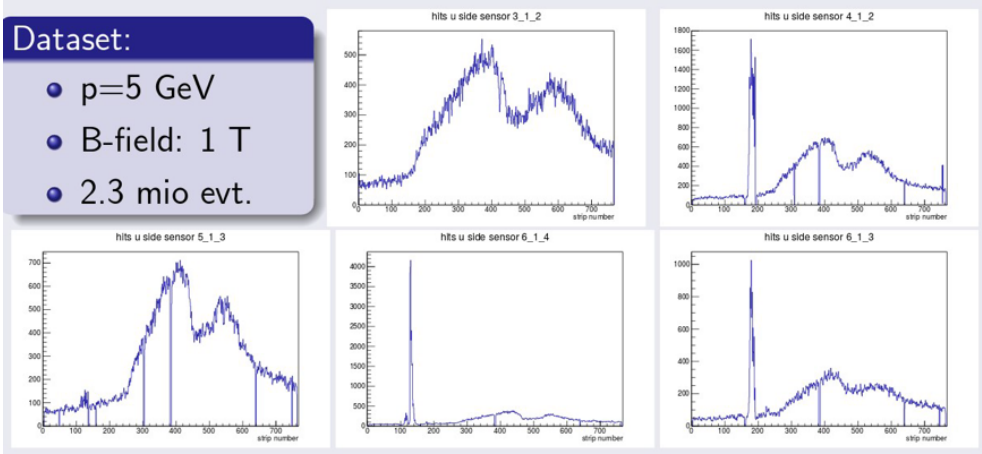

Figure 4-8: examples of hit-map in 2016 TB data set

Chapter 5

Ghost hits reduction analysis

The main purpose of using data from test beam is to most closely approximate the environment of real experiment when SuperKEKB and Belle II mount up isn't fully prepared. The ghost hist reduction just as discussed in Chapter 3, is requested by the requirement of fast online tracking for PXD ROIs determination. From Belle experience, inner layer 3 (L3) draws particular attention when estimating ghost rates due to its position. So driven by this, this study lays an emphasis on data collected on L3, which is about 1.5% ghost rate, equally speaking 100 ghost hits. In TB data, most of ghost hits are filtered by tracking algorithm in reconstruction, so we approximately assume that hits from TCs or Tracks on L3 are all treated as the record of true hits in order to retrieve the charge correlation.

For the purity study and searching of formula of possibility density of ghost hits s, the ghost hits simulation is based on simple statistical assumption that identical event random variable is equivalent to the distribution of simultaneous multiple events.

Because this topic is the first one that is focusing on charge information of correlation in SVD, it provides an excellent chance for estimating the simulation accuracy in detail. VXD simulation plays a significant role in full Belle II simulation so that it must be satisfyingly correct. By compared the beam test data and simulation based on same run environment, the validation of simulation can be testified. What's more, calibration of SVD still remain unclear and problematic because of the difficulty of hardware test such as gain alignment and electronics parameters measurement.

Through the comparison, offline calibration becomes possible if we finely adjust the simulated parameters that are contributing to signal sides. This can be undoubtedly useful when actual gain alignment in strip level is inadequately accurate.

Simulation of test beam is packaged in "testbeam" in master branch of basf2 and for offline analysis, a featured branch called "testbeam_Feb2017" on the server is checked out. Expected goals for the analysis can be itemized as follows:

1. Study of asymmetry or symmetry of P&N charges VS. cluster sizes for both TB and simulation.

2. Charge collection efficiency study for P&N sides, offline calibration feasibility study.

3. 2D charge distribution of TB data and simulated ghost hits purity check, searching for P.D.F distribution.

4. Spacepoint optimization $\rightarrow$ more sophisticated cuts.

5.1 Charge correlation and offline calibration

Electrons and holes produced inside of SVD silicon sensors will be absorbed driven by electronic field to the strips, coupled to capacitance and shapers to form output signals in ADC modules. In this process, electrons and holes could be re-combined, affected by heat noise and blocked by output threshold. These factors may cause loss of signals weight, fluctuation of amplitudes, and biased signal (such as single strip signal). Intrinsically, noise of strips on each sensor is not calibrated and defected strips can make random fake signals. But in general, a physics hit from real particle will naturally generate same amount of charges in the excitation of silicon. So the output of signals are expected to be concentrated to some extend. The deviation of two side signals actually reveals the affections of all interfering process by diffusing the charge deposition.

As for present data restore, analyzer can get access to all recorded all clusters built from digital signals. The stored information in "SVDClusters" including charge, seed

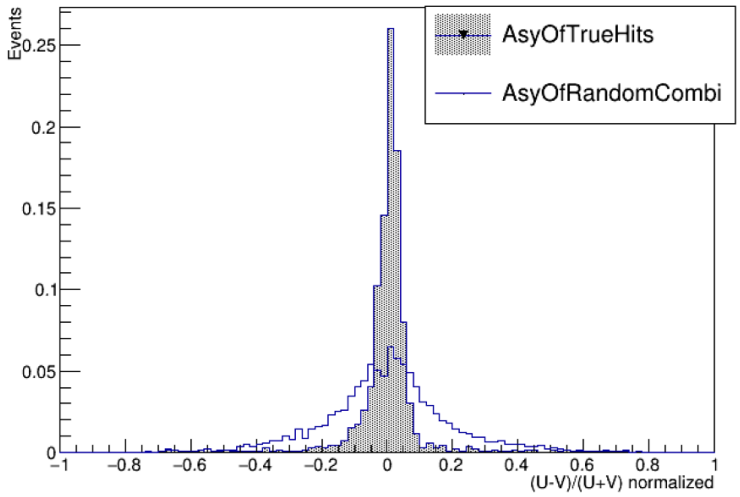

Figure 5-1: truehits from simulation shows the possible concentration against random P and N combination

charge, charge error, position, cluster time and so on, basically everything about energy. And charge collected of clusters is that summed from all strips in one cluster and converted as ADC unit count number. One thing that has to be noticed is ADC count for charge collection is not calibrated for experiment yet. It's believed to be about 10 to 15 percent divergence. So simulation can help to calibrated offline as well by matching TB and simulation data.

Reconstruction is the first step to build offline data to analyze. The featured reconstruction script is provided in steering files for basf2 and it requires users to configure the specific options according to the environments used in data set from TB, such as event number, magnet field, geometry of detectors, momentum of beam and so on. Considering the efficiency of code execution and statistical confidence, feasibility study should use a proper sized data set. So in my case, runs with 30$\sim$ 50 thousands events do the best, taking within 10 minutes in reconstruction.

After reconstruction, TCs are built and relationship between these data structure are assigned. SVDClusters will be spawned from SVDDigits, and TCs as hit lists, indicate which clusters in the SVDClusters are associated with TCs. On the other hand, simulation will additionally restore branches of simulated variables like SVDTrueHits and SVDSimHits, because Geant4 uses them to simulate the energy

Run	#Event	Beam Energy	Magnet	Geometry
168	32757	4.0 GeV	OFF	2PXD[3]

deposition in silicon sensor and response from electronics readout. Also, relations from these variables in simulation to reconstructed ones are available for analysis. [1]

To define a variable presenting the correlation of charges on P and N sides, asymmetry seems a decent choice which stands for "the difference of P and N charge divided by the sum of them". It ranges from $-1 \sim +1$ and presents the deviation of charge collection on both sides. In a perfect matching situation that no fluctuation occurs, this value shall be zero.

$$Asy = \frac{Q_P - Q_N}{Q_P + Q_N} \tag{5.1}$$

In reconstruction of tracks, there are multiple cut can be set for filtering event, since in each event there may be more than one TCs passing the reconstruction, but the first one is best fitted. So we only select first TC in those events who has at least one successfully reconstructed track. For hit filtering, once we have the hits used in TCs, only L3 hits with exact one P strip and one N strip are taken into next step analysis, no single side cluster allowed. [2]

Next step is to dump the physics information from selected hits into minus rootfiles for more various analysis. The asymmetry of P and N charge comes first as mentioned. Here we selected TB run 168 with corresponding simulation.

From Fig 5-3 and 5-4 charges asymmetry of P and N side from TB and simulation shows a consistency on peaking at zero as we expected. It is highly noticeable that distributions form a plain concentration about zero in both TB and simulation results. Moreover, a clear side band appears when Asy is smaller or larger than 0.2. Compared

[1] In terms of relations of variables in basf2 please refer to content of Chapter3 basf2 architecture. Format of data is same for TB and simulation but TB data needs unpacker and TrueHits and SimHits are set null in TB case.

[2] Reconstruction can create single hits in TCs with only one P or N cluster since VXDTF allows single cluster input, but those are useless for our analysis.

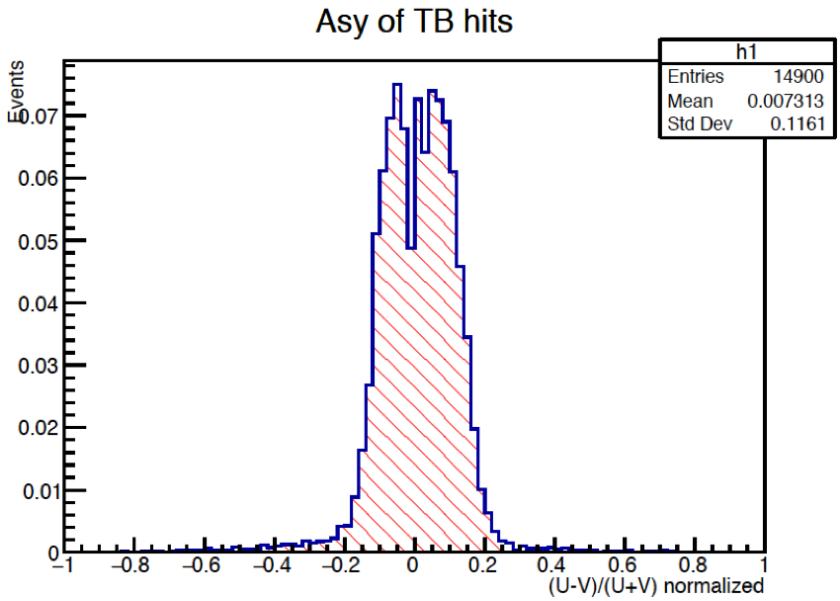

Figure 5-2: Asy of TB run 168

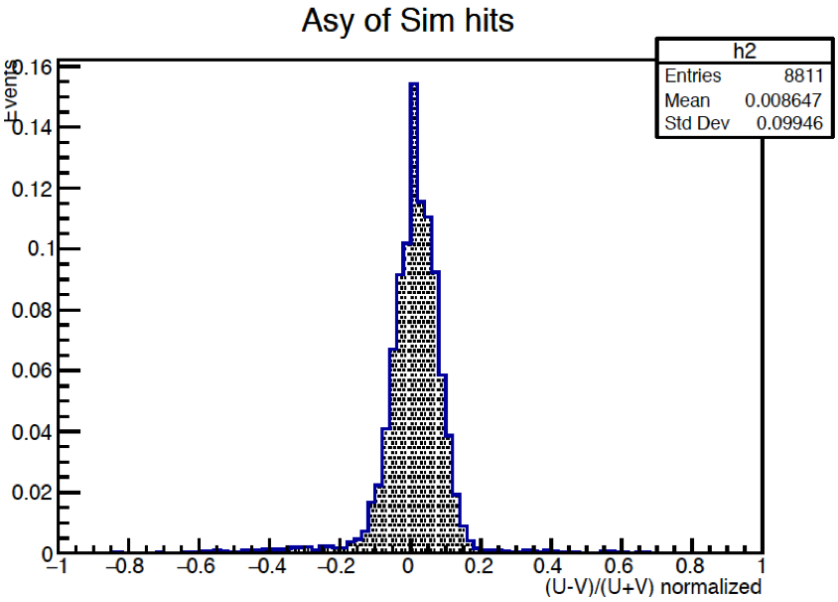

Figure 5-3: Asy of simulated run 168

to the Fig 5-1, side band is quite likely due to the mis-combinations of P and N clusters. While more information needs to be extract from it.

In TB data, larger deviation is shown and small valley structure appears at around zero. This presumably comes from the uncertainty of incident angle of beam line to sensor plane and no calibration of ADC has been applied. What more interesting thing is the Square-Mean-Root difference between TB and simulation that comes from the charge collection efficiency difference of cluster sizes. Asy of hits are affected by charge on P and N side clusters' sizes because we found that the intermediate strips, as known as floating strips, collect charges drastically different depending on P or N sides and cluster sizes. So then Asy for all combinations of cluster sizes on P and N sides are presented in Fig 5-5. (cluster size larger than 2 events only take up lesser than 2%).

Obviously from Fig 5-6, most possible value for Asy deviates from zero in cases of different cluster sizes ratio. When it comes to TB, this pattern get larger. In size-1 N clusters hits, Asy is negatively drifted and in size-2 N clusters hits, the opposite pattern happens. Uniformly, in simulation both deviations are not as significant as that of TB data, which requires further investigation about potential problem in simulation. When looking at specific charge collections on both side VS. cluster sizes, such effect becomes clear. Size-2 clusters gains lesser charge in N side and get overpowered in P side, check Fig 5-7 and 5-8 for detail.

Throughout analyzing the possible source of such deviation between TB and simulation, the major reason is the coupling capacitance wrongly estimated in SVDDigitizer module. Again, the none-zero MPV distribution can result from no calibration of gain and diffusion of beam incidence, but hardware gain calibration remains challenging and unclear to developers to achieve, not to mention that if it's necessary to fix small misalignment. But matching simulation with real experiment is essential and meaningful. By tuning the parameters used in determining SVD readout for clusters with different sizes, the offline calibration is undertaking. For example, from equation 3.1 to 3.5, by adjusting the amplifying coefficient of C_i, the signals of size-2 clusters can be aligned in simulation to approach the distribution of TB data. Equation 5.2

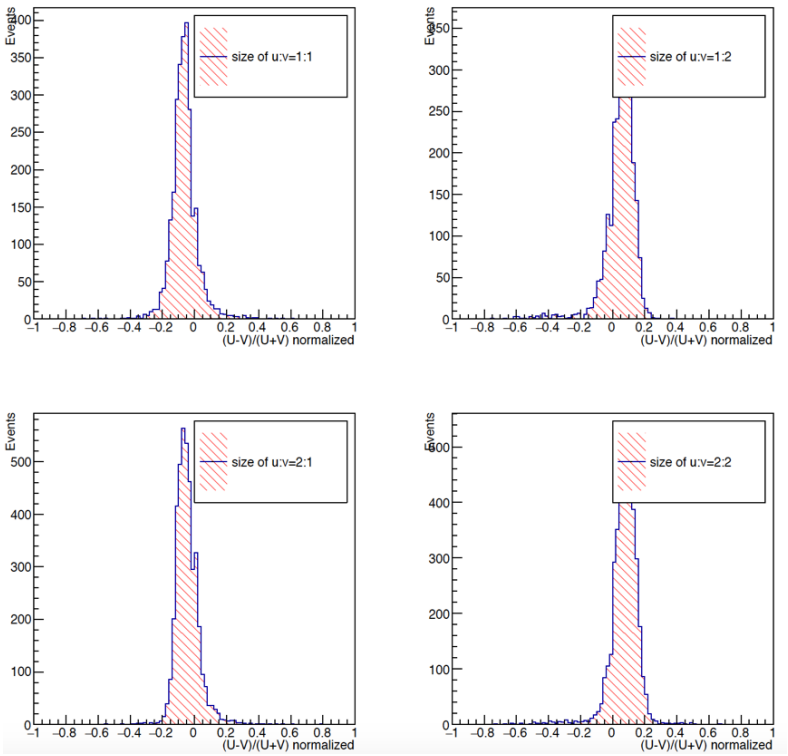

Figure 5-4: Asy of TB regarding P&N cluster sizes ratio (U&V for P&N)

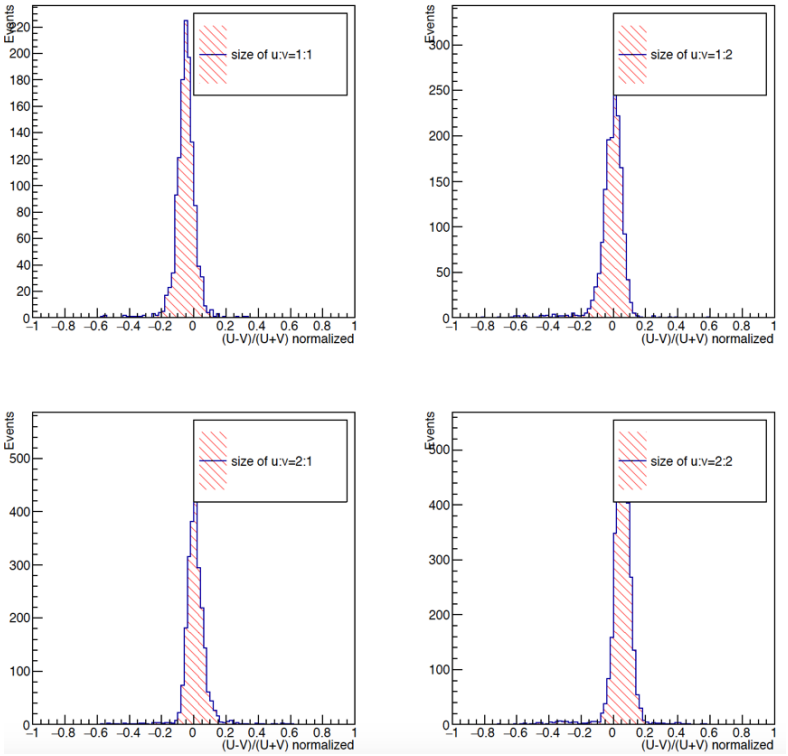

Figure 5-5: Asy of Simulation regarding P&N cluster sizes ratio (U&V for P&N)

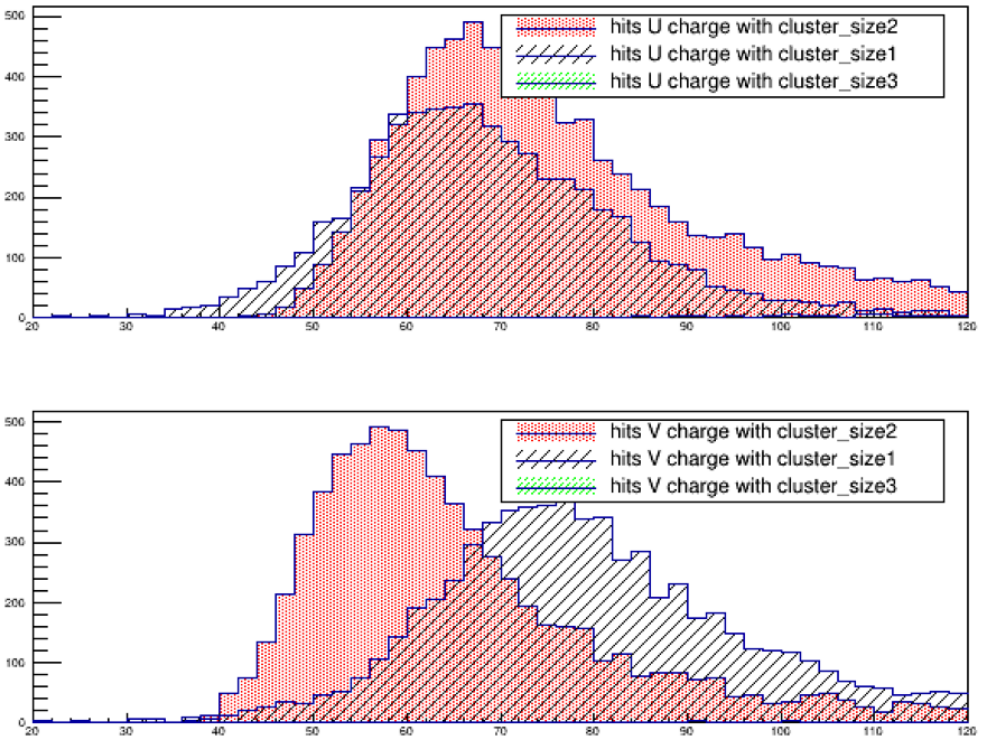

Figure 5-6: charge collection distribution of **TB** VS. cluster size on P&N sides

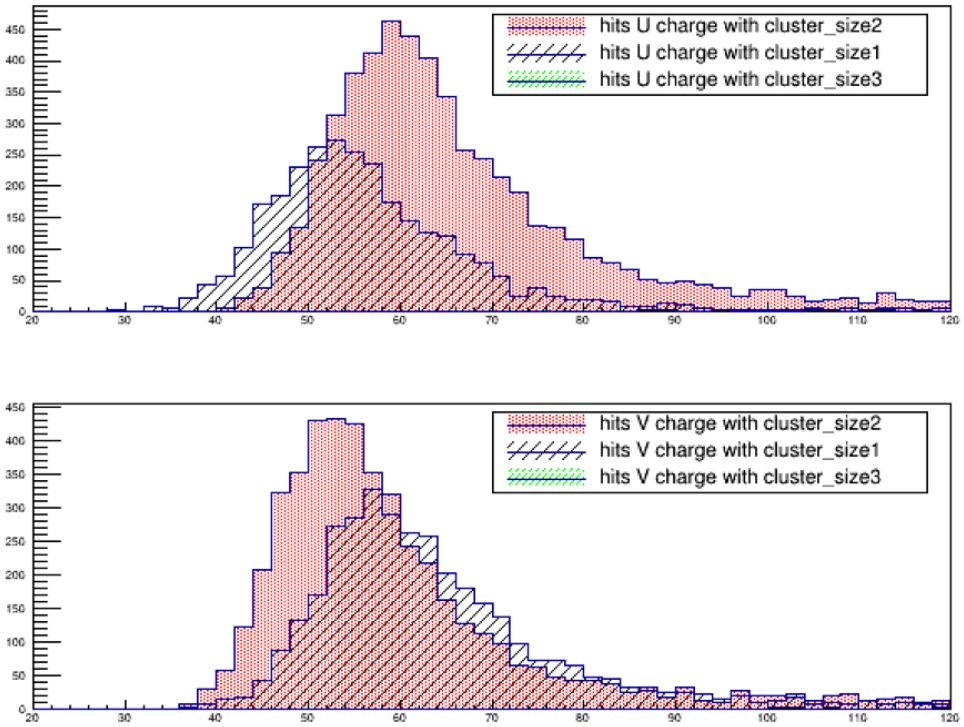

Figure 5-7: charge collection distribution of **simulation** VS. cluster size on P&N sides

shows the ratio of charges from a floating strip coupled into one neighbouring readout strip in SVDDigitizer. The total charges from two adjacent strips should be about 100%, when $C_i \gg C_b$, a should be about 2, but the offset in master branch code is 1 with double overpowered gain. Changing factor a and values for these capacitance can effectively tuning simulation to TB result, like what Fig 5-9 shows. When a is factor of 2, the distribution of charge collection is closer to the TB data but can be improved using more elaborate factor adjust. In same principle, all clusters with different sizes can be aligned using same method with a good feasibility. This work is ongoing with great care of a more sophisticated estimation on coefficients and capacitance.

$$Q_{neighbour} = \frac{C_i}{a \times C_i + C_b} \times Q_{floating} \tag{5.2}$$

5.2 2D charge distribution and purity

Asy is a decent choice for ghost hits reduction if we put a cut on it and test the signal-ghost ratio using MC sample. While Asy is not a direct variable based on cluster charges and might lose some information since it's normalized. Because we assume that VXDTF does a effective filtering for hits then Asy would only contain very small mount of mis-combinations of clusters. Then searching a cut using Asy could cause a large signal loss even if it's done right.

Rather than taking risk in losing true hits, more practical method is that using true hits data set to simulate ghost hits combinations, and then by assuming the ghost rate estimated from occupancy, a purity P.D.F could be given and utilized as an indicator for true hits. The most direct way to do that is to take 2D charge distribution as the candidate of P.D.F. Still, the analysis takes run 168 data as source. The data set is the collection of all clusters on L3 whom at least one TC is associated to.

The way for ghost hits generation is to randomly choose a cluster on L3 from data set, mark its side, and randomly select another with different event index, and if it's

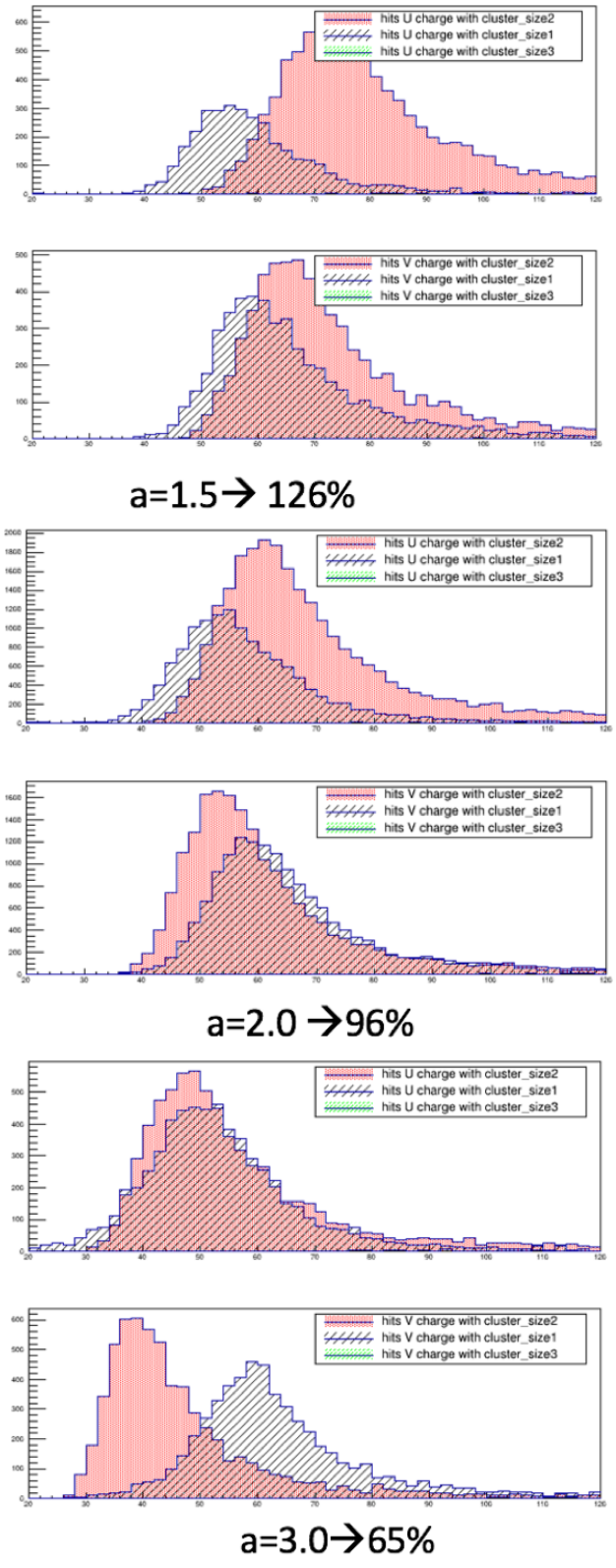

Figure 5-8: Simulation results from different factor of a. Percentage is estimated ratio of "half total" readout (one neighbour) and $Q_{floating}$, $a = 2$ the simulation is closest to TB.

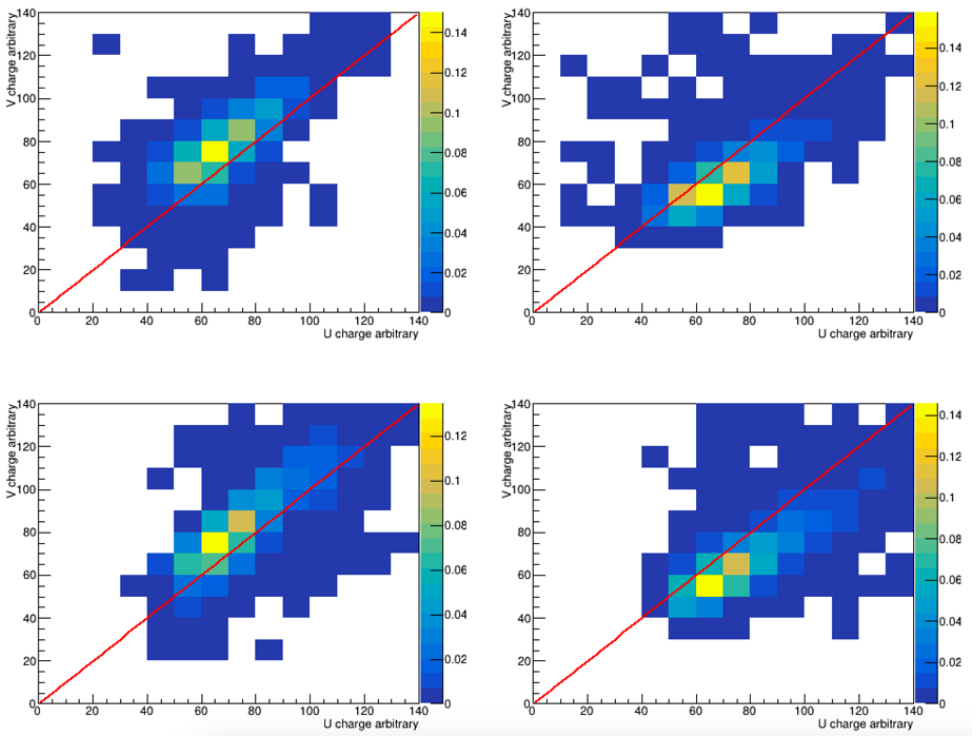

Figure 5-9: 2D charge distribution of Q_P VS. Q_N in **TB** for P size VS. N sizes at Upper left: 1:1, upper right 1:2, bottom left 2:1, and bottom right 2:2

on the opposite side, make two of them a ghost hits, otherwise loop the searching. The ghost hits production can be quite time consuming in this way so the number of ghost hits is set to be lesser, in my case 3000 hits. Undoubtedly, more ghost hits you generate, more accurate ghost distribution you shall get.

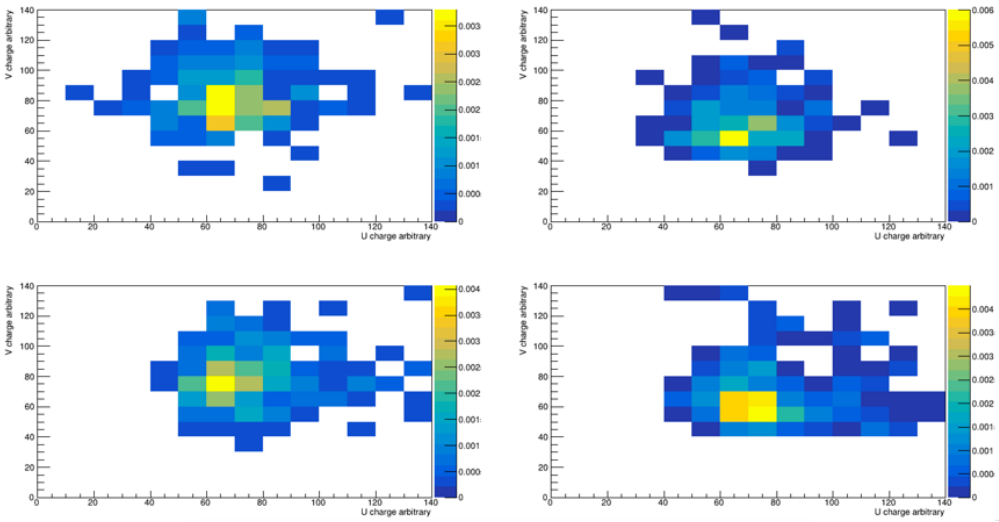

Figure 5-10: 2D charge distribution of Q_P VS. Q_N in **ghost hits** for P size VS. N sizes at Upper left: 1:1, upper right 1:2, bottom left 2:1, and bottom right 2:2. The plot is normalized by all events number with color chart indicating its density.

As expected , the ghost hits distribution shows a much larger divergence compared to the TB data, and the displacement of charges concentration from perfect match line (red line in Fig 5-10) agrees with the result of Asy in section 5.1. It tell us that using 2D charge distribution is feasible in ghost hits recognition. Here, if the assumed ghost rate is set to be 5%, then the Fig 5-10 can be re-scaled and cut off from the Fig 5-9 to get the purity as P.D.F, see Fig 5-11. Be aware, if the ghost rate estimated from occupancy is changed, the purity will change obviously. The ghost rate from occupancy is actually higher than it' expected to be here, because VXDTF already does the filtering, so this is a strong cut. Also, one must realize that binning should be determined by the amount of hits used in purity analysis to achieve a rather continuously and smoothly distributed contour map. It won't truly affect the result, but is important in defining acceptance region from purity.

The lego view of Fig 5-12 gives a nice candidate of P.D.F. The start point of this

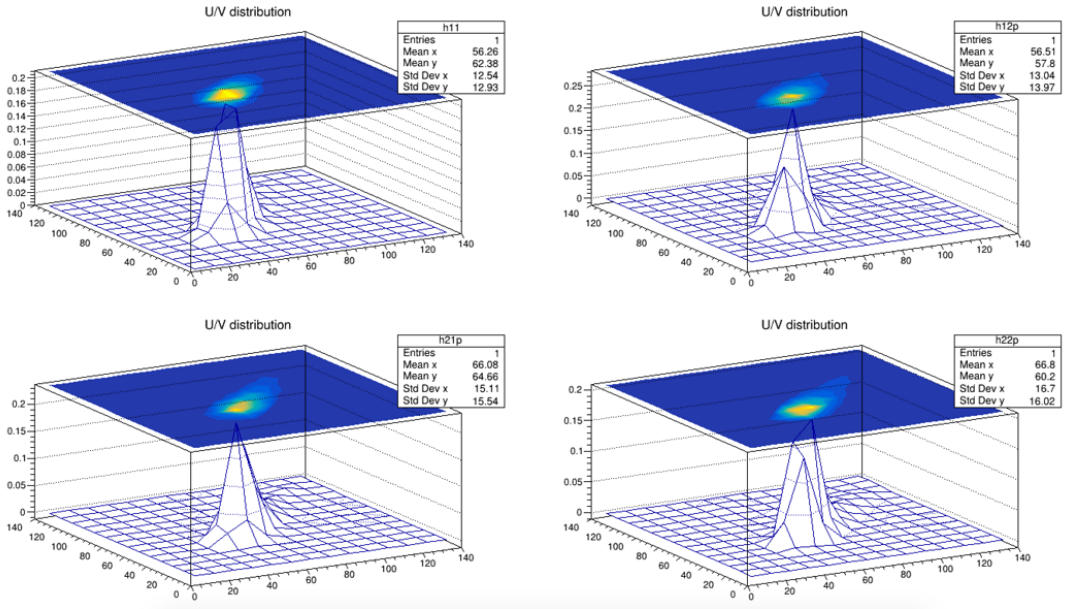

Figure 5-11: Purity of true hits on L3, for P size VS. N sizes at Upper left: 1:1, upper right 1:2, bottom left 2:1, and bottom right 2:2. The plot is normalized by all events number with color chart indicating its density.

TB run 168 L3	P clusters	N clusters
Raw data	77444(2.5/evt)	74616(2.3/evt)
after cut	52364(1.6/evt)	47321(1.4/evt)
hits on tracks	14900(0.95/evt)	14900(0.95/evt)
signal left	13991(0.89/evt)	13991(0.89/evt)
acceptance	SPs reduced 60%	signal loss 6.1%

feasibility study is to reject ghost hits in SpacePoint creation stage for fast tracking. With the purity distribution, we can assign a weight value from Fig 5-12 to any possible combination in SP creation, given their ratio of cluster sizes. For instance, we only send those clusters combination which are located in a specific region in purity to the SP creator. Even though there is a possibility of signal loss by applying such cut, the P.D.F value can be added as part of data set, then let the offline analyzer choose how to use them independently. Here, 3000 simulated ghost hits are generated by choosing hitsontracks randomly on both sides, and ghost rate after reconstruction is assumed at around 5%. Based on the purity distribution, charge regione are set to be 45 to 90 on P side and 40 to 90 on N side, covering the most of reconstructed hits.

By calculating how many spacepoints we can reduce from the all possible combinations, the SPs reduction fraction can be known. Also, the fraction of ghost hits in this cut and signal loss are easy to obtain. In this case, about 5.75 SPs are created per event and only 2.31 are considered to remain with the cut. In the data after reconstruction, about 6.1% hits are still located inside the region. 98% hits that are filtered are ghost hits.

Chapter 6

Conclusion

To achieve the official run of Belle II and operation of SuperKEKB in late 2018, many work has been tirelessly done with such great passion from our collaborators. The Phase II and III test are on scheduled in 2017 which also requires the preparation of subgroups demanding. SVD ladder assembly as well as software optimization play an irreplaceable role in the successful operation of Belle II. The assembly work of SVD must be finished before middle of 2018 and gets ready for Phase III test. The software optimization has to be guaranteed before end of 2017.

The gratifying is that a effective procedures for SVD assembly is well-established and reinforced. The quality of SVD ladders is assured by both mechanical estimation and electronics test thanks to the comprehensively developed process as we discussed in Chapter 2. In the meanwhile, SVD online and offline software are also making surprising progress in optimization. The basf2 architecture becomes more stable and powerful after dozens of version upgrades, and to further boost its online performance to cope with high event rates in Belle II, the feasibility study of ghost hits reduction is undergoing and already achieves a constructive result at present stage.

We have validated the fundamental effectiveness of SVD simulation in beam test environment. In charge correlation study, the highly correlated pattern of charge collection from two sides of DSSD sensors is discovered, which is affected by the sizes of clusters. This provides a chance for offline calibration of gain in software. To closely check the possibility of rejecting ghost hits, 2D charge distribution and

purity are presented by artificially generating ghost hits using reconstructed hits on tracks. The purity study shows a high feasibility of taking charge correlation as a criterion in hits filtering, giving us confidence to further explore the potential of the method in next step.The analysis is only partially cover those tracks that hit the DSSD sensors roughly perpendicular, and in real experiment will generate various tracks with broader angular range. So does the energy deposition. This will lead to much more wrong combinations of two side signals, giving our method more power on filtering than it appears to be in TB data. Surely, this should be explored and confirmed in Phase II and Phase III test. At present, the topic is under the supervision and direction of SVD software group.

However, there are still many challenges and more we can do ahead of our work. For instance, data set used in charge correlation study can be enlarged to check the consistence of the distribution, More data set being taken in can surely benefits the accuracy. And the result of that under active magnet field for low momentum beam should be taken care of since there will be more large size clusters. In addition, purity is presented in contour map now but the attempt of its parameterization is worthy. All related work above for in-depth optimization has been started and methodically carried forward when finishing this thesis.

Appendix A

SVD hardware

In this part of appendix, the SVD hardware information and assembly will be included for further understanding of the experiment.

A.1 SVD assembly

The overall structure of SVD consists of ladder's support, silicon sensors and electronics materials. Given the restrictive bugdet and the requirements of B Physics, the Origami concept, the sensors on the supporting ribs and end ring hybrid structure are designed. Two composite sandwich carbon fiber ribs (SCFR) are glued to the Origami sensor area in such a way that no structure interferes with the bond wires on the sensor side and shorts are avoided. To strengthen the stability of double end of electronics hybrid, another reinforcement of of ribs is attached with one layer of carbon fiber to have more stiffness in the joint area with the endring mount structure.

Since the hardware work I mainly participated is in the assembly of SVD L6, so the procedure of actual ladder assembly will be briefly described in the work of L6 group. Be awared of the difference of assembly between different layers, the detail can be varied.

The whole assembly process is a finely designed, practically tested procedure that experienced many corrections and has been proven successful to meet the requirements mentioned before. The L6 ladder is composed of forward, backward, OCE (center)Z±

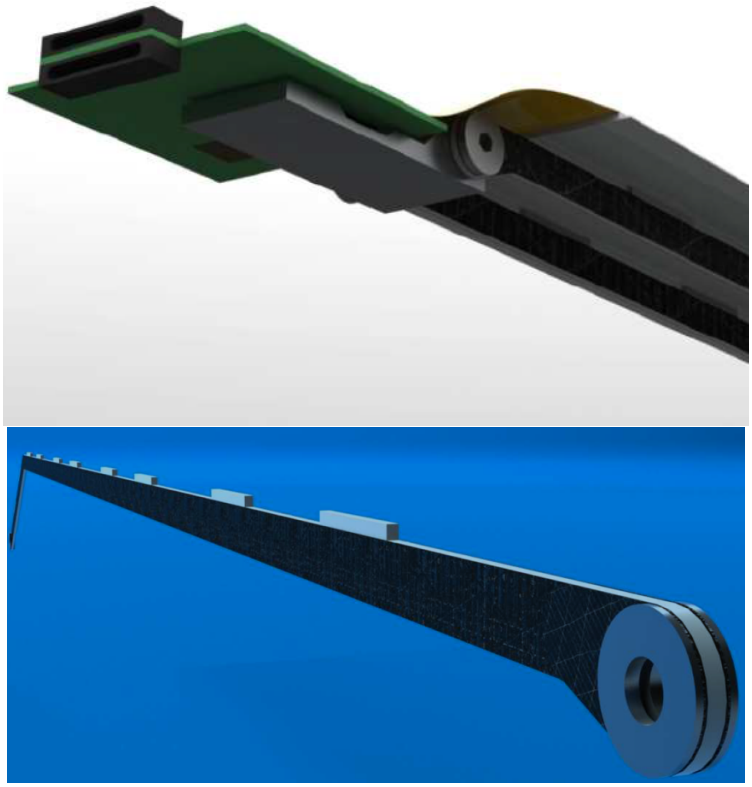

Figure A-1: Ladder of L6 scheme of sandwich composed rib (bottom) and endring mounts with hybrid board (top).

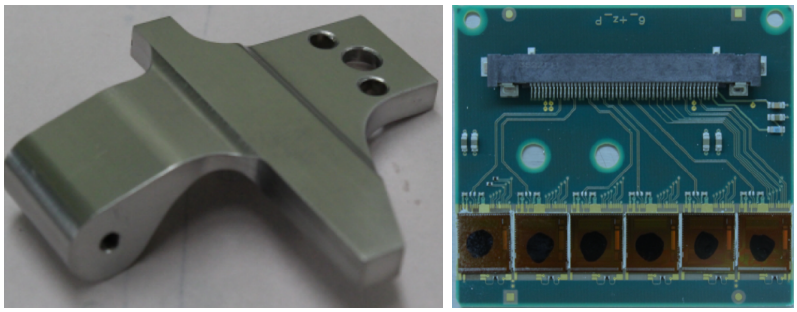

Figure A-2: electronics hybrid board (right)and end mount supportor (left) of SVD L6

.

and Origami modules. And the general assembly procedure has following steps:

- Gluing of DSSD sensors with RA to the assembly bench which plays the role as a location lock and assembling platform in the whole process.

- Placement of five DSSDs with alignment in a very high spatial precision, guranteed by the F mark (seal on the corner of each sensor) microscope check.

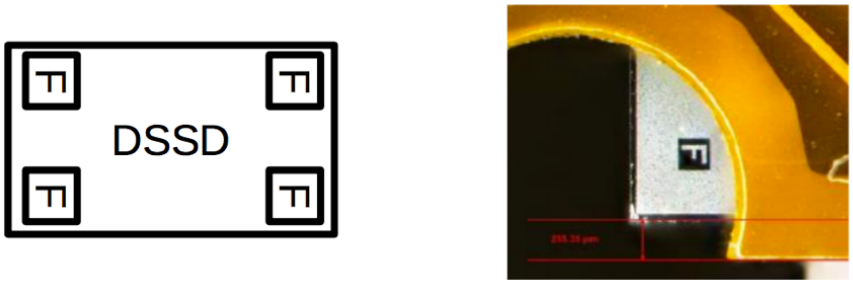

Figure A-3: F mark on sensors' corner for position check

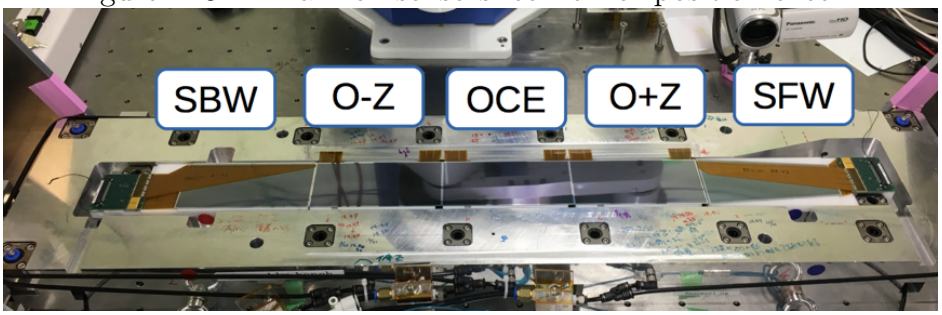

Figure A-4: Rough placement of DSSDs on assembly bench before the Origami gluing

- Backward and forward DSSDs are glued to rib with the pitch adapters and wire bond. OCE and Z± (three modules) are glued to the Origami after the alignment.

- Then the PA1 and PA2 at the corner of sensor will be wrapped to the other side of sensors and glued to the area of Origami where the APV25 channels are fan out prepared to bond with.

- Finally step is to combine the half ladder and the supporting structure (rib) and lock the screws.

After the mechanical production of a ladder, the precsion check starts. First, the displacements of ladders on three directions are checked using CMM platform, which assures the quality of mechanical performance. Then, taking advantage of the dark box in the clean room and data aquisition system, the electronic performance of ladder can testified. When a ladder passes the quality check, it will be carefully packed and stored in the shelter for further use. For those that can not be used in real experiment or beam test, they will be either abandoned or kept for assembly procedure validation purposes based on to what extend they are damaged or deformed.

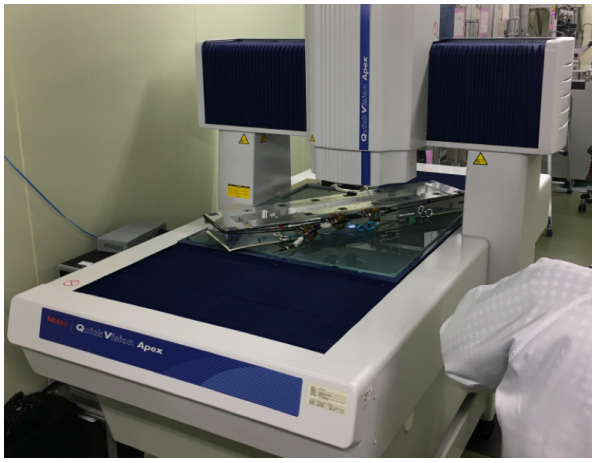

Figure A-5: CMM measurement platform

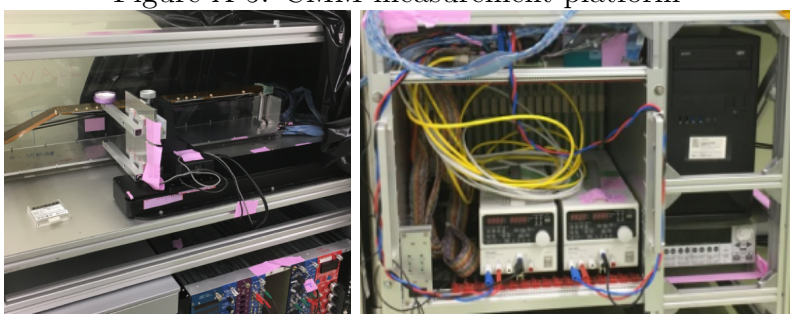

Figure A-6: Chamber for electronics and source test(left),Data Aquisition computers(right)

The detailed assembly procedures including common assembly, Origami Modules assembly, gluing and wire bonding are not the main body here. Since Spring of 2016, after several runs of assemly procedures study and practice, massive production of SVD L6 was offically started. By April of 2017, nine ladders of L6 have been manufactured and four passes the quality assurance that allows them to be used in

real experiment. The first ladder was shipped to DESY, Germany for 2016 and 2017 beam test. In future, there will be 20 working ladders for L6. Approximately, one ladder assembly and test takes up for 15 days, so by the end of Nov. of 2018, the whole massive production of SVD shall be finished if no more expected issues occurs.

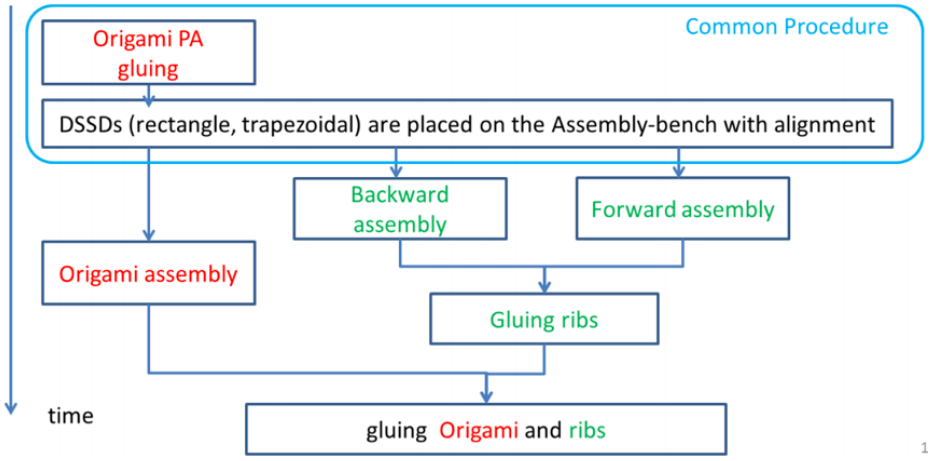

Figure A-7: Timing of assembly of SVD L6 procedures

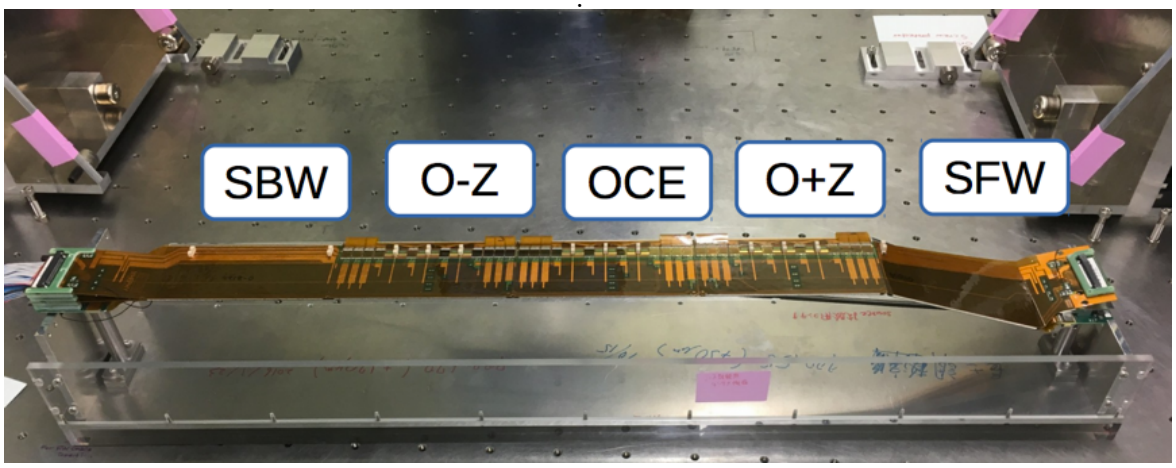

Figure A-8: Finished ladder of L6

Quantity	Large Sensors	Small Sensors
# strips P side	768	768
# strips N side	512	768
# floating strips P side	767	767
# floating strips N side	511	767
Area(total)	7442.85 mm^2	5048.90 mm^2
Area(active)	7029.88 mm^2(94.5%)	4737.80 mm^2(93.8%)

Table A.1: Basic parameters of rectangular sensors

Quantity	Value
Base material	Si n-type 8kω
Full depletion voltage FD	$<$ 120V
Breakdown voltage	$\geq$50V+FD
Polysilicon resistor	$4M\Omega$(Min.) 10MΩ(typ.)
Coupling capacitance	$>$100pF
Breakdown voltage of AC coupling	$>$20 V
Bias leak current at FD	$1\mu A$ (typ.) $10\mu A$ (Max.)

Table A.2: Electrical parameters of rectangular sensors

Quantity	Value
# strips P side	768
# strips N side	512
# floating strips P side	767
# floating strips N side	511
Area(total)	6382.6 mm^2
Area(active)	5890 mm^2(92.3%)
Slant angles	Layer 6 : 21.1°
	Layer 5: 17.2°
	Layer 4: 11.9°

Table A.3: Basic parameters of the trapezoidal sensor.

Quantity	Value
Base material	Si n-type 8kΩcm
Full depletion voltage FD	40V(Min.) 70V(Max.)
Operation voltage	FD $\sim$ 2FD
Breakdown voltage	$\geq$ 2.5FD
Polysilicon resistor	10MΩ, 15$\pm$5 MΩ
Interstrip resistance, p-side	100MΩ(Min.) 1GΩ(typ.)
Interstrip resistance, n-side	10MΩ(Min.) 100MΩ(typ.)

Table A.4: Electrical parameters of rectangular sensors

Appendix B

Figures

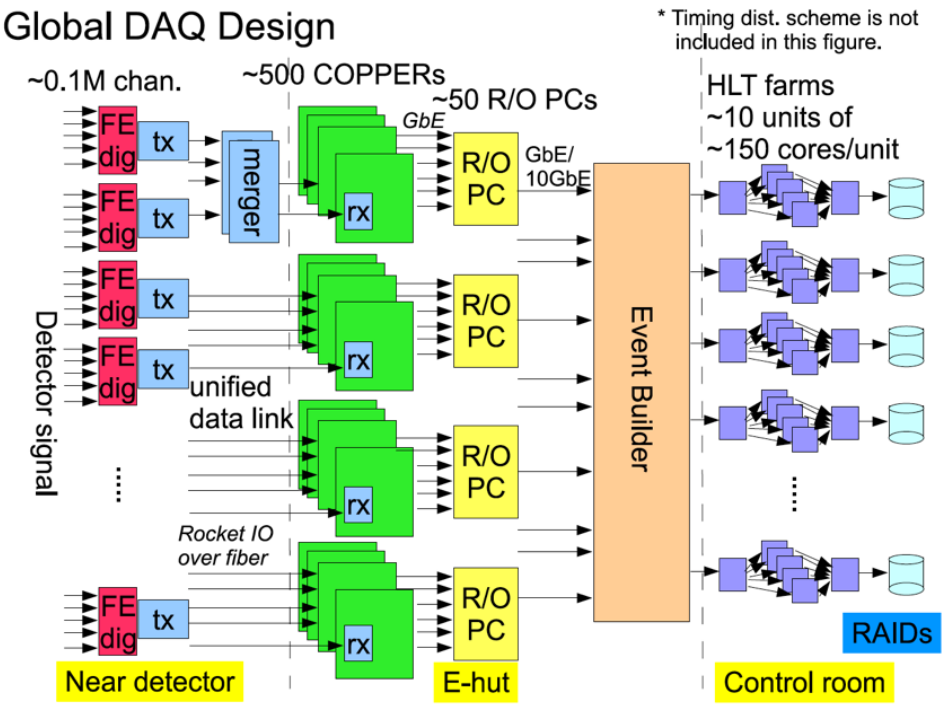

Figure B-1: Conceptual design of Belle II DAQ system.

It's noticed that the ROI determination is highly dependent on alignment geometry accuracy. Fig B-3 is an example of different alignment used in global track fitting and their difference.

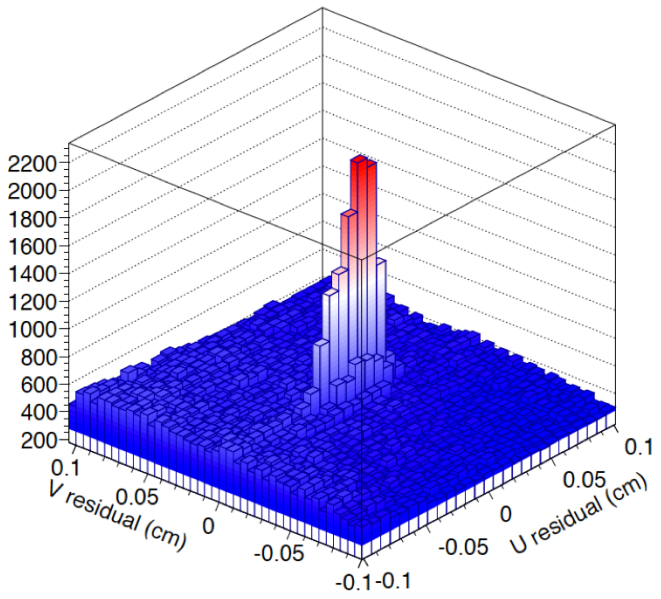

Figure B-2: Residual between the intercept of the reconstructed SVD tracks on the PXD plane and the actual PXD hits for 1000000 test beam events. The bins match the PXD pixels. A Gaussian fit estimates the width of the central peak as $32.3 \pm 0.4 \mu m$ and $141 \pm 2 \mu m$ in the V and U directions, respectively. Here U denotes the bending direction

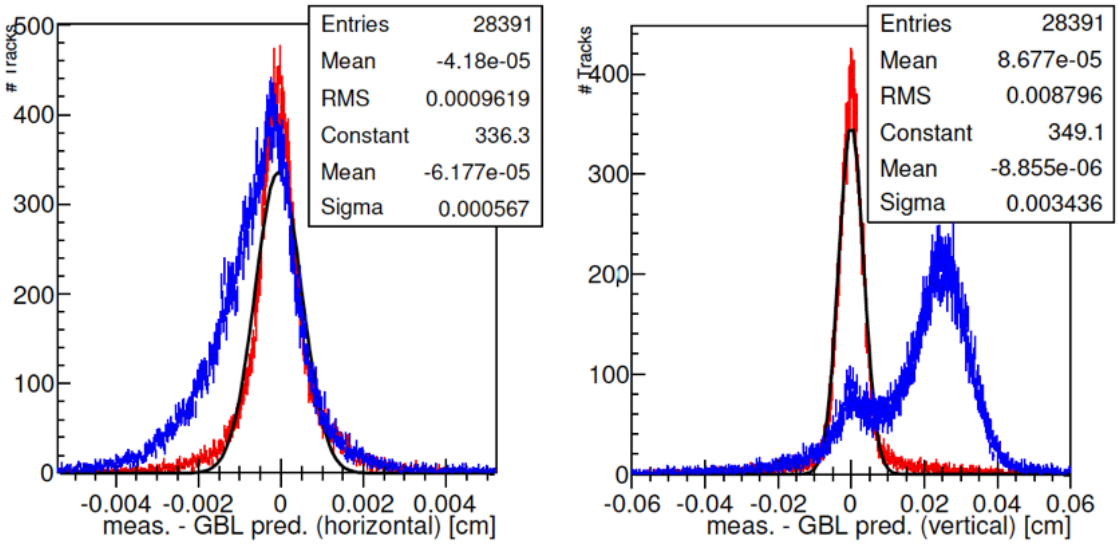

Figure B-3: GBL refit residuals in V (left) and U (right) directions of the second SVD sensor using nominal (blue) and aligned (red) geometry. Parameters of a Gaussian fit (black curve) to the red histogram are given.

Bibliography

[1] Steven Weinberg. The making of the standard model. *The European Physical Journal C-Particles and Fields*, 34(1):5–13, 2004.

[2] Nicola Cabibbo. Unitary symmetry and leptonic decays. *Physical Review Letters*, 10(12):531, 1963.

[3] James H Christenson, Jeremiah W Cronin, Val L Fitch, and Rene Turlay. Evidence for the 2 π decay of the k 2 0 meson. *Physical Review Letters*, 13(4):138, 1964.

[4] Ashton B Carter and Anthony I Sanda. Cp nonconservation in cascade decays of b mesons. *Physical Review Letters*, 45(12):952, 1980.

[5] Kazuo Abe, R Abe, I Adachi, Byoung Sup Ahn, H Aihara, M Akatsu, G Alimonti, K Asai, M Asai, Y Asano, et al. Observation of large cp violation in the neutral b meson system. *Physical Review Letters*, 87(9):091802, 2001.

[6] Tsung-Dao Lee and Chen-Ning Yang. Question of parity conservation in weak interactions. *Physical Review*, 104(1):254, 1956.

[7] The ckm quark-mixing matrix. `http://pdg.lbl.gov/2014/reviews/rpp2014-rev-ckm-matrix.pdf`.

[8] Y. Amhis et al. Averages of b-hadron, c-hadron, and τ-lepton properties as of summer 2016. 2016.

[9] Hai-Yang Cheng, Chun-Khiang Chua, and Amarjit Soni. Effects of final-state interactions on mixing-induced c p violation in penguin-dominated b decays. *Physical Review D*, 72(1):014006, 2005.

[10] H Koiso. Design of superkekb based on the nano-beam scheme. 2010.

[11] T Abe, I Adachi, K Adamczyk, S Ahn, H Aihara, K Akai, M Aloi, L Andricek, K Aoki, Y Arai, et al. Belle ii technical design report. *arXiv preprint arXiv:1011.0352*, 2010.

[12] M. Raymond. Apv25 power consumption. 2006.

[13] for Belle II Software Group Tobias Schlter. Vertexing and Tracking Software at Belle II . 2014.

[14] T. Geler, W. Khn, J. S. Lange, Z. Liu, D. Mnchow, B. Spruck, and J. Zhao. The onsen data reduction system for the belle ii pixel detector. *IEEE Transactions on Nuclear Science*, 62(3):1149–1154, June 2015.

[15] Johannes Rauch and Tobias Schlüter. Genfita generic track-fitting toolkit. In *Journal of Physics: Conference Series*, volume 608, page 012042. IOP Publishing, 2015.

[16] B Chopard and M Droz. *Cellular automata*. Springer, 1998.

[17] Rudolf Frühwirth, Robin Glattauer, Jakob Lettenbichler, Winfried Mitaroff, and Moritz Nadler. Track finding in silicon trackers with a small number of layers. *Nuclear Instruments and Methods in Physics Research Section A: Accelerators, Spectrometers, Detectors and Associated Equipment*, 732:95–98, 2013.